Chapter 7

Peer-to-Peer Energy Transactions in Real-Time Scenarios Using the Kalai-Smorodinsky Bargaining Model

7.1 Introduction

In the earlier chapters, various techniques were used for modeling the energy management system. But they all focus on the day-ahead scheduling. In real-time scheduling, the modelling of a battery energy storage system is complicated, along with maintaining the grid constraints. This chapter incorporates the real-time scheduling of various buildings along with the battery energy storage systems with the help of day-ahead scheduling. This work also illustrates the effect of integrating the distribution network constraints in energy management systems. The main contribution of this chapter can be summarised in the following way.

- A P2P energy trading framework based on KS bargaining solution is proposed in this chapter without violation of network constraints. Also, this framework considers DSO and DGs to be actively participating in the energy market.

- For enhancing the practicality of the proposed work, a two-tiered energy-sharing framework is proposed where one focuses on day-ahead energy scheduling while the other deals the real-time market operations. Also, validating this work from a real-time digital simulator (RTDS) enhances its feasibility.

- This work deals with the intermittency of renewable energy resources in the real-time energy market by incorporating the BESS in real-time with the help of the receding horizon method.

Besides the aforementioned, this framework takes into account the impact of uncertainties concerning RESs. The escalating number of prosumers heightened the burden on both communication infrastructure and computational complexity [65]. These limitations are also dealt with in this work by means of a virtual community (VC).

7.2 Energy Trading Without Consideration of Distribution Network Constraints

In this section, the problem is formulated without considering the distribution network parameters. These constraints are incorporated in the problem formulation later in section 7.3.

7.2.1 Problem Formulation

This section discusses the problem of the various elements involved in the system architecture.

7.2.1.1 System Architecture

In this work, the VCs are formed by grouping all the neighbouring buildings and a BESS (Figure 7.1). A separate and secure platform is also present to facilitate the energy exchange among building-to-building (B2B), building-to-community (B2C), and community-to-community (C2C). This platform is specially designed for cloud computing and limited information sharing so that all the coupling decisions are well dealt with. This concept is used to reduce the communication and computational burden associated with P2P energy trading without compromising any of the related advantages.

7.2.1.2 Building Model

The cost function, $C^{B}_{n,i}$, of i^{th} building of n^{th} community can be written as shown below.

$$C^{B}_{n,i} = \sum_{t=1}^{T} C^{LS}_{n,i,t} + C^{b2b}_{n,i} + C^{b2c}_{n,i}, \tag{7.1}$$

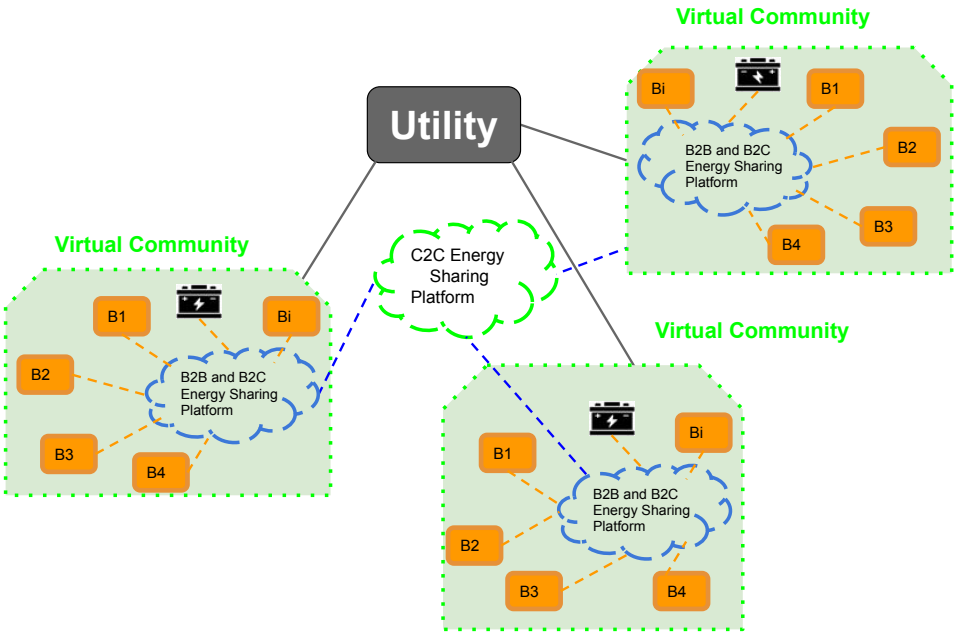

Figure 7.1: SCHEMATIC DIAGRAM OF PEER-TO-PEER ENERGY TRADING

where,

$$C^{LS}_{n,i,t} = \Lambda^{disc}_{t}(P^{LS}_{n,i,t} - L^{A}_{n,i,t})^2, \tag{7.2}$$

$$C^{b2b}_{n,i} = \sum_{j=1,\ j\neq i}^{N^B_n} \pi^{b2b}_{n,i,j}, \text{ and} \tag{7.3}$$

$$C^{b2c}_{n,i} = \pi^{b2c}_{n,i}. \tag{7.4}$$

Here, $C^{LS}_{n,i,t}$, $C^{b2b}_{n,i}$, $C^{b2c}_{n,i}$ are the discomfort cost due to load shifting, energy trading cost in B2B, and B2C, respectively. And Λ^{disc}_{t}, $L^{A}_{n,i,t}$, and $P^{LS}_{n,i,t}$ are the discomfort cost coefficient, load before shifting and load after shifting, respectively. In B2B trading, $P^{b2b}_{n,i,j,t}$, or B2C trading, $P^{b2c}_{n,i,t}$, energy imports will be treated as positive, while in the case of exports will be considered negative. Similarly, the positive values of incentives ($\pi^{b2b}_{n,i,j}$ and $\pi^{b2C}_{n,i}$) indicate that building is paying. The incentives are used to motivate the prosumers such that,

$$C^{B0}_{n,i} - C^{B}_{n,i} \geq 0. \tag{7.5}$$

The $C^{B0}_{n,i}$ refers to the cost of the building without P2P trading. The other constraints associated with buildings are as follows.

$$L^{min}_{n,i,t} \leq P^{LS}_{n,i,t} \leq L^{max}_{n,i,t}, \tag{7.6}$$

$$\sum_{t=1}^{T} P^{LS}_{n,i,t} \geq \epsilon^{LS} \sum_{t=1}^{T} L^{A}_{n,i,t}. \tag{7.7}$$

$$P^{b2b}_{n,i,j,t} + P^{b2b}_{n,j,i,t} = 0, \qquad \text{and} \tag{7.8}$$

$$\pi^{b2b}_{n,i,j} + \pi^{b2b}_{n,j,i} = 0. \tag{7.9}$$

The equation (7.6) and (7.7) are associated with load shifting, i.e., maximum/minimum limit and load curtailment, respectively. Since the constraints (7.8) and (7.9) has variable of both i^{th} and j^{th} buildings of n^{th} VC, therefore they are coupling constraints. The load balancing equation for each building can be given by the following.

$$-\sum_{j=1,\ j\neq i}^{N^B_n} P^{b2b}_{n,i,j,t} - P^{b2c}_{n,i,t} = R_{n,i,t} - P^{LS}_{n,i,t}. \tag{7.10}$$

7.2.1.3 Virtual Community Model

The cost function of a virtual community (C^c_n) consists of the cost involved in energy exchange with the utility ($C^U_{n,t}$), battery utilization cost ($C^{BESS}_{n,t}$), and the cost occurred due to energy exchange with other VCs (C^{c2c}_n). Thus,

$$C^c_n = \sum_{t=1}^{T}(C^U_{n,t} + C^{BESS}_{n,t}) + C^{c2c}_n, \tag{7.11}$$

where,

$$C^U_{n,t} = (\Lambda^{im}_{n,t} + \epsilon^{CE})P^b_{n,t} - \Lambda^{ex}_{n,t}P^s_{n,t}, \tag{7.12}$$

$$C^{BESS}_{n,t} = \Lambda^{UTI}(P^{ch}_{n,t} + P^{dis}_{n,t}), \quad \text{and} \tag{7.13}$$

$$C^{c2c}_n = \sum_{m=1,\ m\neq n}^{N^C} \pi^{c2c}_{n,m}. \tag{7.14}$$

Here, $P^b_{n,t}$, $P^s_{n,t}$, ϵ^{CE}, $\Lambda^{im}_{n,t}$, and $\Lambda^{ex}_{n,t}$ are the power import and export from the utility, charges due to carbon emission, power import price, and power export price respectively. $P^{ch}_{n,t}$ and $P^{dis}_{n,t}$ are the charging and discharging power of BESS and Λ^{UTI} is the BESS utilization coefficient. Inter-community power exchange ($P^{c2c}_{n,m,t}$) is considered as positive for import and negative for export. Similarly, the incentive ($\pi^{c2c}_{n,m}$) is positive when the VC is paying, else it will be negative. Since in this work, the virtual community is considered to be a non-profit-based entity, the total cost of VC is distributed to the buildings as follows.

$$C^c_n = \sum_{i=1}^{N^B_n} \pi^{b2c}_{n,i}. \tag{7.15}$$

And the related constraints are as follows.

$$SOC_{n,t} = (1 - \eta_n^{loss}) SOC_{n,t-1} + \eta_n^{ch} P_{n,t}^{ch} - \frac{1}{\eta_n^{dis}} P_{n,t}^{dis}, \tag{7.16}$$

$$P_n^{ch_{min}} \leq P_{n,t}^{ch} \leq P_n^{ch_{max}}, \tag{7.17}$$

$$P_n^{dis_{min}} \leq P_{n,t}^{dis} \leq P_n^{dis_{max}}, \tag{7.18}$$

$$SOC_n^{min} \leq SOC_{n,t} \leq SOC_n^{max}, \tag{7.19}$$

$$P_{n,m,t}^{c2c} + P_{m,n,t}^{c2c} = 0, \tag{7.20}$$

$$\pi_{n,m}^{c2c} + \pi_{m,n}^{c2c} = 0, \tag{7.21}$$

$$C_n^{c0} - C_n^c \geq 0, \qquad and \tag{7.22}$$

$$P_{n,t}^b - P_{n,t}^s + P_{n,t}^{dis} - P_{n,t}^{ch} + \sum_{\substack{m=1 \\ m \neq n}}^{N^C} P_{n,m,t}^{c2c} = \sum_{i=1}^{N_n^B} P_{n,i,t}^{b2c}. \tag{7.23}$$

The next stage, SOC, is defined by equation (7.16). For limiting the charging power, discharging power, and state of charge ($SOC_{n,t}$), equation (7.17),(7.18), and (7.19) is used respectively. The equation (7.20) and (7.21) are the constraints related to the C2C energy exchange. For promoting the C2C energy exchange, equation (7.22) is used where the cost of each VC with no C2C energy exchange is given by C^{c0}. The load balancing equation for VC is given by (7.23), with the number of VCs being equal to N^C. This framework doesn't need any separate constraints to prevent simultaneous charging and discharging or buying and selling to the grid, as explained in Appendix III.

7.2.2 Methodology

The cooperative game theory is used for the energy trading between buildings and virtual communities. The uncertainties related to the RESs are handled using Hong's 2p point estimate method (PEM) [77] as described in Section 2.9. In subsequent sections, only the cost function is denoted by $\mathbb{E}(.)$ instead of all variables for simplicity.

For the model described in section 7.2.1, a cooperative game is formulated whose nash equilibrium is calculated with the help of a modified nash bargaining problem (MNBP), known as Kalai–Smorodinsky (KS) bargaining solution [84]. The cooperative game can be described as given in Table 7.1. The game is played in two levels due to the presence of B2C coupled variables.

Table 7.1: DESCRIPTION OF THE COOPERATIVE GAME

Levels	Players	Strategies	Objectives
1	Buildings	$X^{B}_{n,i,t}$:=($P^{LS}_{n,i,t}$, $P^{b2b}_{n,i,j,t}$, $P^{b2c}_{n,i,t}$, $\pi^{b2b}_{n,i,j}$, $\pi^{b2c}_{n,i}$)	$C^{b}_{n,i}$
2	VCs	$X^{c}_{n,t}$:= ($P^{b}_{n,t}$, $P^{s}_{n,t}$, $P^{ch}_{n,t}$, $P^{dis}_{n,t}$, $P^{c2c}_{n,m,t}$, $\pi^{c2c}_{n,m}$)	C^{c}_{n}

And the required MNBP is

$$\mathscr{F}_1 : \ max[\prod_{n=1}^{N^C}\{\prod_{i=1}^{N^B_n}(\mathbb{E}(C^{B0}_{n,i}) - \mathbb{E}(C^{B}_{n,i}))(\mathbb{E}(C^{c0}_{n}) - \mathbb{E}(C^{c}_{n}))\}]. \tag{7.24}$$

subject to:

$$\mathbb{E}(C^{B0}_{n,i}) - \mathbb{E}(C^{B}_{n,i}) = K^{b2b}_{n,i}(\mathbb{E}(C^{B0}_{n,i}) - \mathbb{E}(C^{B*}_{n,i})), \tag{7.25}$$

$$\mathbb{E}(C^{c0}_{n}) - \mathbb{E}(C^{c}_{n}) = K^{c2c}_{n}(\mathbb{E}(C^{c0}_{n}) - \mathbb{E}(C^{c*}_{n})), \tag{7.26}$$

$$K^{b2b}_{n,i} = K^{b2b}_{n,j}, \quad j = 1, 2....N^B_n \tag{7.27}$$

$$K^{c2c}_{n} = K^{c2c}_{m}, \quad m = 1, 2....N^C. \tag{7.28}$$

Here, the expected cost in the best case is given by $\mathbb{E}(C^{B*}_{n,i})$ and $\mathbb{E}(C^{c*}_{n})$ where the energy bought/sold from/to peers at a price equal to that of selling/buying energy to/from utility respectively. For ensuring fair incentive distribution, the variables $K^{b2b}_{n,i}$ and K^{c2c}_{n} are used such that the ratio of optimal cost reduction and best cost reduction is the same for each peer. Thus, the strategies of buildings and VCs will include $K^{b2b}_{n,i}$ and K^{c2c}_{n} also. For each iteration, $C^{B*}_{n,i}$ and C^{c*}_{n} are calculated using the values of the previous iteration and, thus, are considered as fixed for the present iteration. This is done to maintain the convexity of the objective functions. The (7.24) is a maximization problem and can be converted into a minimization problem as follows.

$$\mathscr{F}_2 : \ min[-\sum_{n=1}^{N^C}\{\sum_{i=1}^{N^B_n} log(1 + \mathbb{E}(C^{B0}_{n,i}) - \mathbb{E}(C^{B}_{n,i})) + log(1 + \mathbb{E}(C^{c0}_{n}) - \mathbb{E}(C^{c}_{n}))\}]. \tag{7.29}$$

By decoupling the coupling constraints:{(7.8), (7.9), (7.20), (7.21), (7.23), (7.15), (7.27), and (7.28)} using alternating direction method of multipliers (ADMM) [76], the problem (7.29) can be solved in a decentralized way. This requires the auxiliary variables ($\sigma^{P_{b2b}}_{n,i,j,t}$, $\sigma^{\pi_{b2b}}_{n,i,j}$, $\sigma^{P_{c2c}}_{n,m,t}$, $\sigma^{\pi_{c2c}}_{n,m}$, $\sigma^{P_{b2c}}_{n,i,t}$, $\sigma^{\pi_{b2c}}_{n,i}$, σ^{K}_{n} and $\sigma^{K^{c2c}}_{n}$) employed for $P^{b2b}_{n,i,j,t}$, $\pi^{b2b}_{n,i,j}$, $P^{c2c}_{n,m,t}$, $\pi^{c2c}_{n,m}$, $P^{b2c}_{n,i,t}$, $\pi^{b2c}_{n,i}$, $K^{b2b}_{n,i}$, and K^{c2c}_{n}, respectively. Thus, the coupling constraints are reformulated as follows.

$$\sigma^{P_{b2b}}_{n,i,j,t} + \sigma^{P_{b2b}}_{n,j,i,t} = 0, \tag{7.30}$$

$$\sigma^{\pi_{b2b}}_{n,i,j} + \sigma^{\pi_{b2b}}_{n,j,i} = 0, \tag{7.31}$$

$$\sigma^{P_{c2c}}_{n,m,t} + \sigma^{P_{c2c}}_{m,n,t} = 0, \tag{7.32}$$

$$\sigma^{\pi_{c2c}}_{n,m} + \sigma^{\pi_{c2c}}_{m,n} = 0, \tag{7.33}$$

$$\sigma^{K^{b2b}}_{n,i} = \sigma^{K^{b2b}}_{n,j}, \quad j = 1, 2....N^B_n \tag{7.34}$$

$$\sigma^{K^{c2c}}_{n} = \sigma^{K^{c2c}}_{m} \quad m = 1, 2....N^C \tag{7.35}$$

$$P^b_{n,t} - P^s_{n,t} + P^{dis}_{n,t} - P^{ch}_{n,t} + \sum_{\substack{m=1 \\ m\neq n}}^{N^C} P^{c2c}_{n,m,t} = \sum_{i=1}^{N^B_n} \sigma^{P_{b2c}}_{n,i,t}, \qquad and \tag{7.36}$$

$$C^c_n = \sum_{i=1}^{N^B_n} \sigma^{\pi_{b2c}}_{n,i}. \tag{7.37}$$

Based on these decoupled constraints, the equation (7.29) can be re-defined as shown below.

$$\begin{aligned}
\mathscr{F}_3 :\ min[-\sum_{n=1}^{N^C}\{\sum_{i=1}^{N^B_n} log(1 + \mathbb{E}(C^{B0}_{n,i}) - \mathbb{E}(C^B_{n,i})) \\
+ log(1 + \mathbb{E}(C^{c0}_n) - \mathbb{E}(C^c_n))\}] + \sum_{n=1}^{N^C}\sum_{i=1}^{N^B_n}[\sum_{\substack{j=1 \\ j\neq i}}^{N^B_n}\{\sum_{t=1}^{T}\frac{\delta_1}{2}(P^{b2b}_{n,i,j,t} \\
- \sigma^{P_{b2b}}_{n,i,j,t} + \frac{\omega^{P_{b2b}}_{n,i,j,t}}{\delta_1})^2 + \frac{\delta_2}{2}(\pi^{b2b}_{n,i,j} - \sigma^{\pi_{b2b}}_{n,i,j} + \frac{\omega^{\pi_{b2b}}_{n,i,j}}{\delta_2})^2\}+ \\
\frac{\delta_{12}}{2}(K^{b2b}_{n,i} - \sigma^{K^{b2b}}_{n,i} + \frac{\omega^{K^{b2b}}_{n,i}}{\delta_{12}})^2] + \sum_{n=1}^{N^C}\sum_{i=1}^{N^B_n}[\sum_{t=1}^{T}\frac{\delta_3}{2}(P^{b2c}_{n,i,t} - \\
\sigma^{P_{b2c}}_{n,i,t} + \frac{\omega^{P_{b2c}}_{n,i,t}}{\delta_3})^2 + \frac{\delta_4}{2}(\pi^{b2c}_{n,i} - \sigma^{\pi_{b2c}}_{n,i} + \frac{\omega^{\pi_{b2c}}_{n,i}}{\delta_4})^2]+ \\
\sum_{n=1}^{N^C}[\sum_{\substack{m=1 \\ m\neq n}}^{N^C}\{\sum_{t=1}^{T}\frac{\delta_5}{2}(P^{c2c}_{n,m,t} - \sigma^{P_{c2c}}_{n,m,t} + \frac{\omega^{P_{c2c}}_{n,m,t}}{\delta_5})^2 + \frac{\delta_6}{2}(\pi^{c2c}_{n,m} - \\
\sigma^{\pi_{c2c}}_{n,m} + \frac{\omega^{\pi_{c2c}}_{n,m}}{\delta_6})^2\} + \frac{\delta_{56}}{2}(K^{c2c}_n - \sigma^{K^{c2c}}_n + \frac{\omega^{K^{c2c}}_n}{\delta_{56}})^2].
\end{aligned} \tag{7.38}$$

The σ, ω, and δ are auxiliary variables, dual multipliers, and penalty parameters, respectively. For the above problem, variables are X^B, X^c, and σ; And the constraints are γ_B :=[(4.3) to (7.5), (7.10),(7.25)], γ_c :=[$P^B \geq 0$, $P^s \geq 0$, (7.17) to (7.19), (7.22), (7.36),(7.37),(7.26)], γ_1 :=[(7.30), (7.31),(7.34)], and γ_2 :=[(7.32), (7.33),(7.35)]. The complete decentralized

energy scheduling is presented in the flowchart shown in Figure 7.2. The ω and δ, are updated as follows.

$$\omega(\tau+1) = \omega(\tau) + \delta(\tau)(X(\tau+1) - \sigma(\tau+1)), \tag{7.39}$$

$$\delta(\tau+1) = \begin{cases} \frac{\delta(\tau)}{\nu}, & \text{if } \lambda^P < \kappa\lambda^D, \\ \nu\delta(\tau), & \text{if } \lambda^P > \frac{\lambda^D}{\kappa}, \\ \delta(\tau), & \text{otherwise.} \end{cases} \tag{7.40}$$

Here the primal residual (λ^P) and dual residual (λ^D) can be defined as $\lambda^P = ||X(\tau+1) - \sigma(\tau+1)||$, $\lambda^D = ||\sigma(\tau+1) - \sigma(\tau)||$.

7.2.3 Simulation Results

In this work 9 buildings (*Bi*) with different load curves (Figure 7.3(a)) and RESs generations (Figure 7.3(b)) are grouped under three VCs (*VC1*, *VC2*, and *VC3*). The rated capacity of Wind power generation (WPG) and solar power generation (SPG) in Figure 7.3(b) is 100kW and 125kW, respectively. The building in *VC1*, and *B2* and *B3* in *VC2* have the same capacity as shown in Figure 4.6(b). While in the remaining buildings, the installed capacity of WG and SG is 50 kW and 100 kW, respectively. The shared BESS is 200kW, whose charging/discharging power limit is 50kW/h, and the limit for SOC level is given by the range [20%,90%]. The shifting of the load is allowed up to $\pm 10\%$, and the fraction of load supplied (ϵ^{LS}) is 1. Other parameters are mentioned in Table 7.2. The price of import of power from the utility is shown in Figure 4.10(b), and the respective export price is assumed to be in a constant proportion with the import price. For optimization, the GAMS/CONOPT4 solver is used on a laptop with 4 GB RAM and a Core $i3$ 1.20 GHz processor.

The following cases have been studied to prove the effectiveness of the proposed framework.
Case I (Base case): In this event, all the buildings exchange energy with the utility only.
Case II: Buildings share energy with other buildings (B2B) and it's VC (B2C) having a shareable BESS. The VCs are the ones who is exchanging the energy with the utility.
Case III: In addition to the above case, C2C energy exchange is also occurring in this case.

A summary for a cost comparison among all the considered cases is depicted in Table 7.3. The total cost for *VC1*, *VC2* and *VC3* in $Case\ I$ is 335.65 \$, 145.40 \$, and 429.15 \$ respectively. This is the highest compared to the other two cases as in this case the buildings are acting

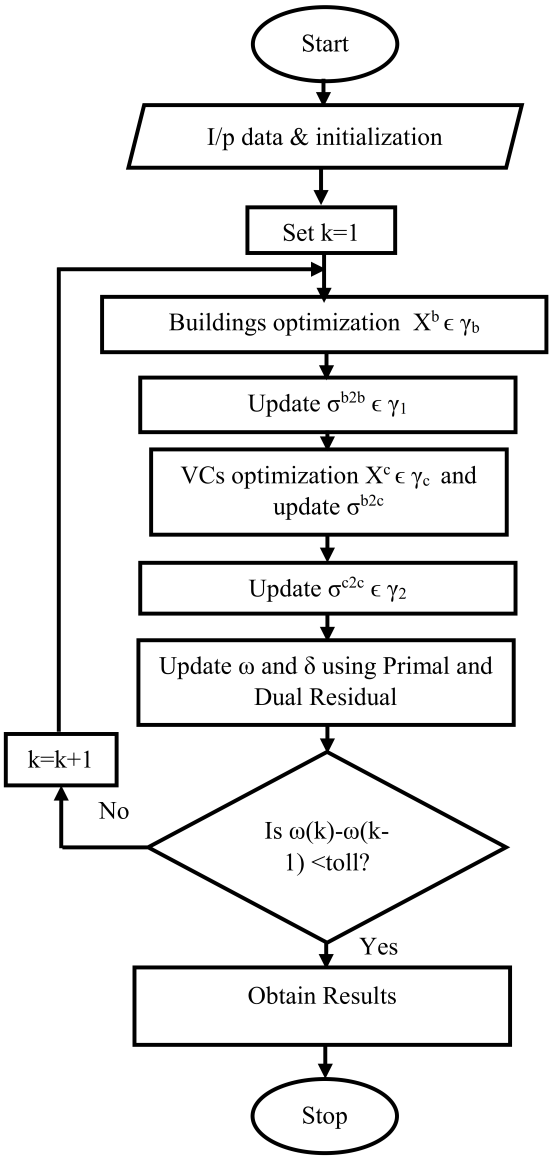

Figure 7.2: FLOWCHART FOR P2P ENERGY TRADING

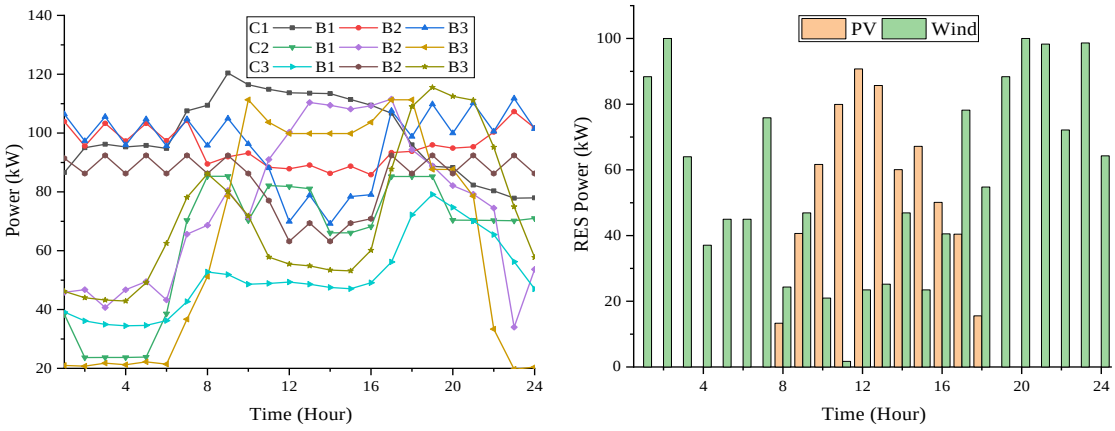

(a) (b)

Figure 7.3: (A) LOAD CURVES OF BUILDINGS (B) RENEWABLE ENERGY SOURCES (RES) POWER GENERATION

Table 7.2: VALUES OF PARAMETERS USED

Parameters	**Values**
η^{ch}	96%
η^{dis}	94.3%
η^{loss}	0.5%
Λ^{UTI}	0.06$/kW
ϵ^{CE}	0.05$/kW
Λ^{dis}	$0.03\$/kW^2$
ϵ_R	4
σ	0.2
κ	0.01
ν	1.5

Table 7.3: COST COMPARISON FOR ALL THREE CASES WITHOUT CONSIDERING DISTRIBUTION NETWORK CONSTRAINTS

		VC1				VC2				VC3			
		B1	**B2**	**B3**	**Sum**	**B1**	**B2**	**B3**	**Sum**	**B1**	**B2**	**B3**	**Sum**
$Case\ I$	C^b	117.71	102.21	115.73	335.65	114.17	23.655	7.58	145.40	57.40	219.76	151.99	429.15
$Case\ II$	C^{ls}	17.78	17.78	16.89	52.46	20.60	24.788	17.88	63.27	12.64	17.34	14.15	44.12
	C^{b2b}	2.99	-5.34	2.35	0.00	37.91	-13.946	-23.96	0.00	-49.50	43.95	5.54	0.00
	C^{b2c}	92.73	87.20	92.12	272.05	39.97	2.750	-5.52	37.20	93.32	154.75	129.50	377.57
	C^b	113.51	99.64	111.36	324.51	98.48	13.592	-11.60	100.47	56.46	216.04	149.19	421.69
$Case\ III$	C^{ls}	0.94	0.94	0.94	2.82	1.44	1.464	1.42	4.32	0.81	0.81	0.81	2.43
	C^{b2b}	2.16	-3.30	1.14	0.00	38.16	-9.910	-28.25	0.00	-44.28	40.10	4.19	0.00
	C^{b2c}	90.50	86.13	89.16	265.79	33.96	2.582	-10.42	26.11	89.51	152.52	126.08	368.11
	C^b	93.60	83.77	91.24	268.61	73.55	-5.864	-37.26	30.43	46.04	193.43	131.07	370.55

independently and meeting their demand through the available RESs generation, load shifting, and exchanging energy with the utility only.

With the availability of energy exchange among buildings (B2B) and BESS in $Case\ II$ and $Case\ III$, the RESs generations are utilised more effectively. This is validated by the decrease in the power exchange with the utility as shown in Figure 7.4. For instance, during 1:00-3:00 hours, the power exported to the utility by *VC2* is reduced in comparison to the base case, as in other cases, this energy is used to charge the battery for use in subsequent hours of the day as shown in Figure 7.5(a). The Figure 7.6 shows the B2B power exchange. *B1* of *VC2* imports power from other buildings during most of the hours of the day and this is the reason why the incentives for B2B trading of this building is positive compared to other buildings as shown in Table 7.3. The surplus/deficit power status of buildings determines the B2B power exchange which then further determines the B2B cost involved. Such energy sharing is beneficial to both sellers and buyers in comparison to the energy exchange with the utility in terms of cost savings.

In $Case\ III$, there is an opportunity of taking benefit of load diversity through C2C power exchange which results in a further decrease in the power export to the utility in comparison to $Case\ II$. The power export to the utility in $Case\ III$ is approximately zero as shown in Figure 7.4(c). In $Case\ III$, for *VC1, VC2* and *VC3* the total cost is decreased by 17.22%, 69.71%, and 12.13% compared to $Case\ II$. The power exchange of buildings with their respective VC is shown in Figure 7.7. In *VC3*, initially, this exchange is the same in both $Case\ II$ and $Case\ III$. But in subsequent hours, the power exported and power imported to/from the VC is increased in

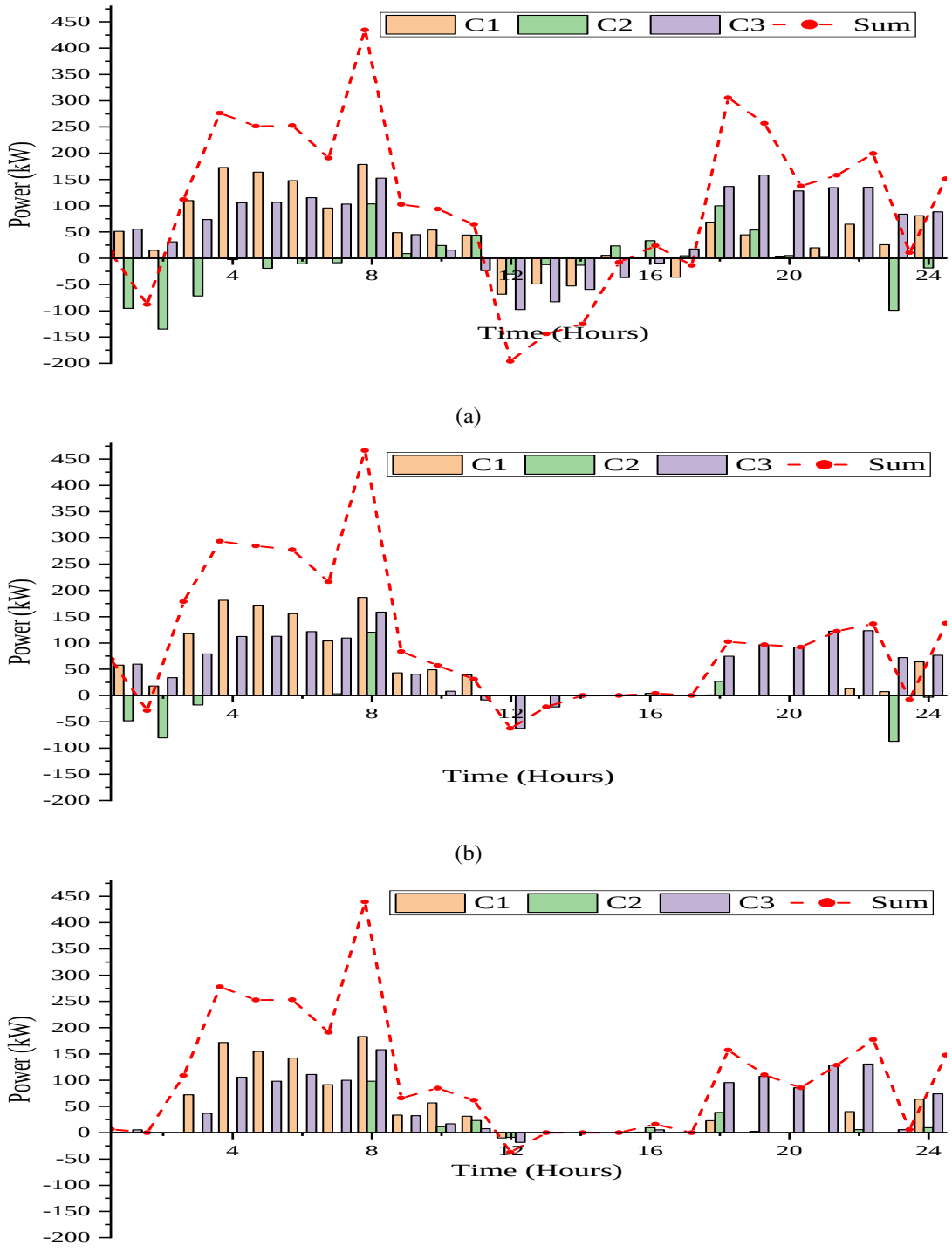

Figure 7.4: Power Exchange of VC with the utility (without consideration of distribution network constraints) (a) *Case I*, (b) *Case II*, (c) *Case III*

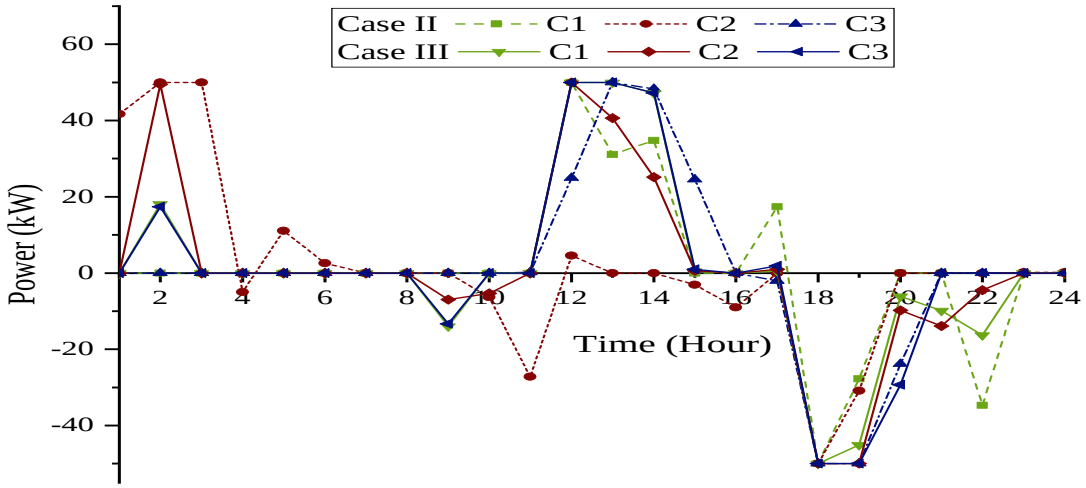

(a)

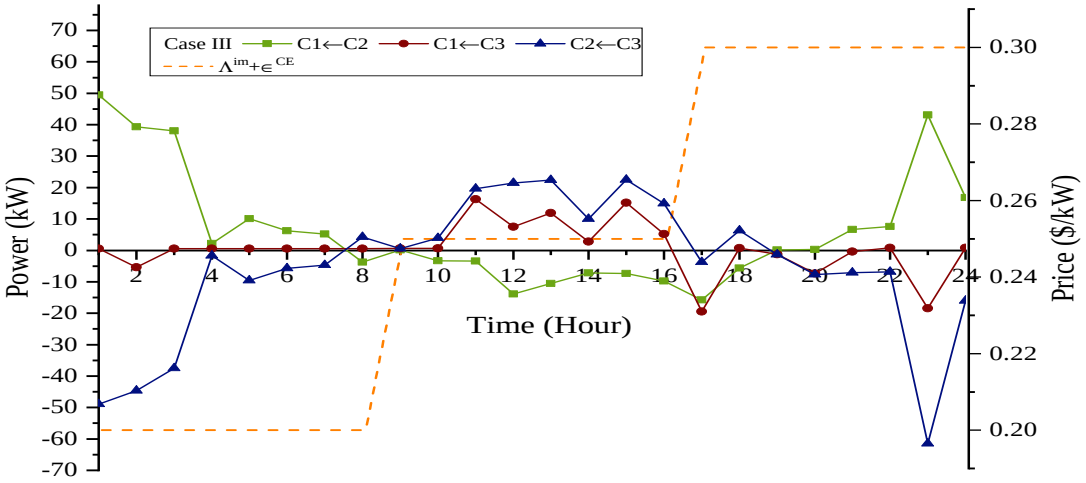

(b)

Figure 7.5: WITHOUT CONSIDERATION OF DISTRIBUTION NETWORK CONSTRAINTS: (A) CHARGE/DISCHARGE POWER OF BESSS (B) POWER EXCHANGE IN C2C ENERGY TRADING

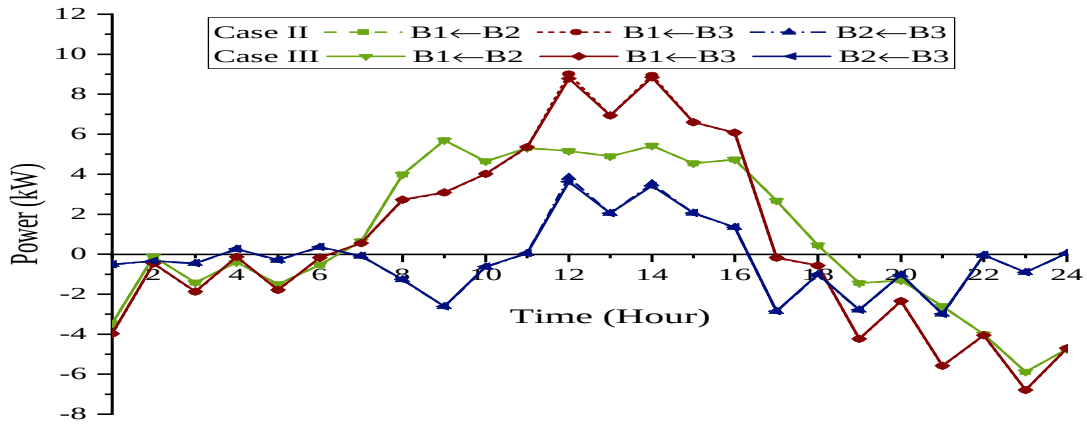

(a)

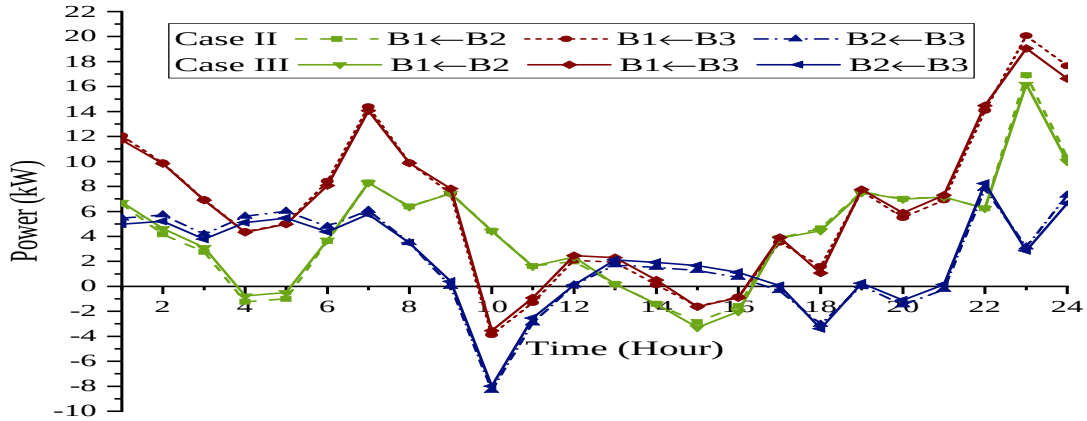

(b)

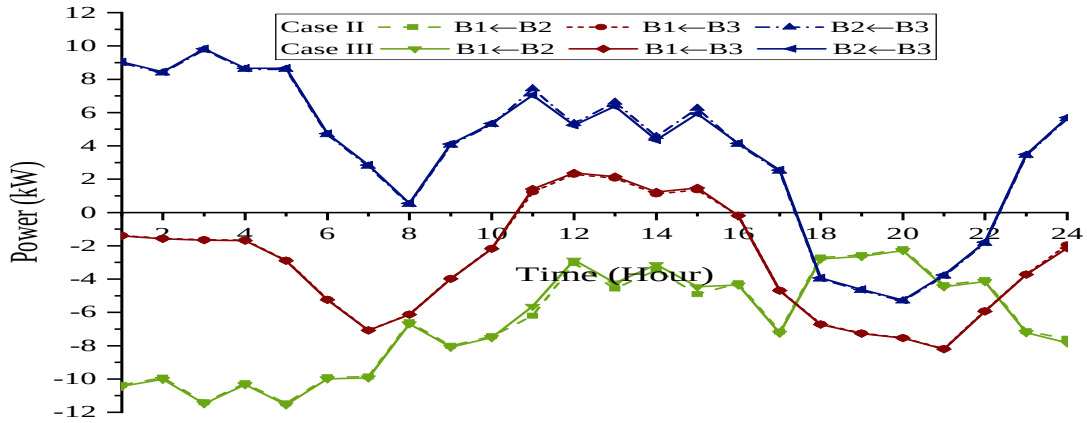

(c)

Figure 7.6: Power Exchange in B2B energy trading (without consideration of distribution network constraints) for *Case II* and *Case III* (a) *VC1*, (b) *VC2*, (c) *VC3*

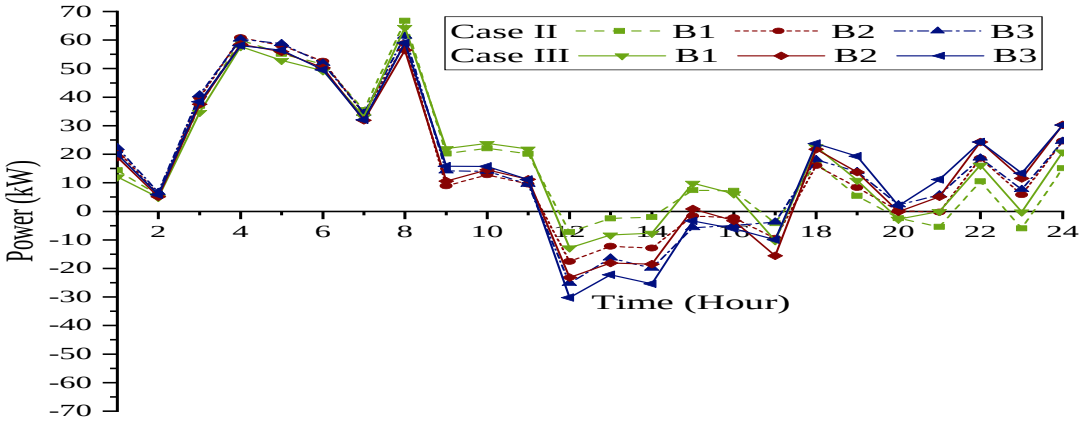

(a)

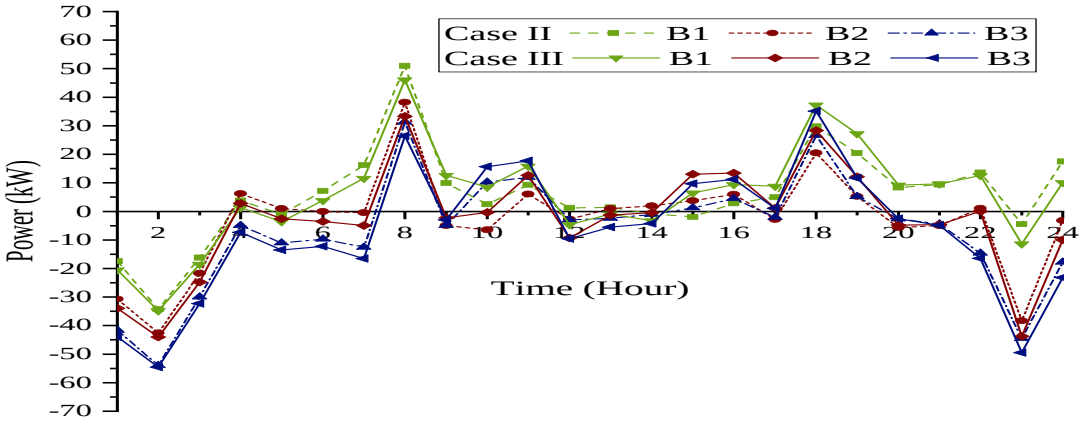

(b)

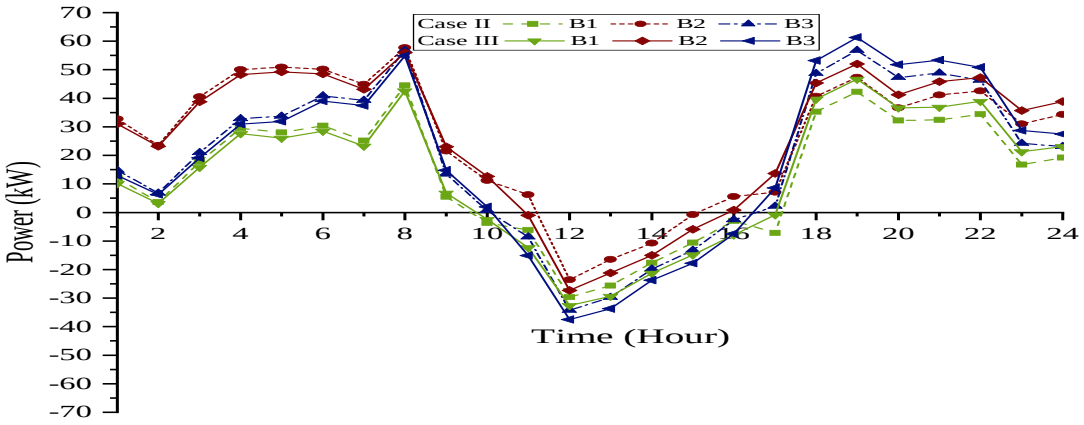

(c)

Figure 7.7: Power Exchange in B2C energy trading (without consideration of distribution network constraints) (a) *VC1*, (b) *VC2*, (c) *VC3*

$Case\ III$ compared to $Case\ II$. This increase in power exchange is due to the presence of the C2C energy trading option. The C2C energy exchange profile is shown in Fig 7.5(b). During 1:00-3:00 hours, *VC2* has surplus energy to export to utility (Figure 7.4(b)) even after charging its battery (Figure 7.5(a)). This surplus power, in $Case\ II$, is then exported to the other VCs in $Case\ III$ as shown in (Figure 7.5(b)).

In $case\ III$, the total C2C incentives for *VC1, VC2*, and *VC3* are 15.92$, -39.64$, and 23.73$ respectively. Only around 11:00-15:00 hours, *VC2* imports power from other VCs (Fig 7.5(b)) for charging the BESS. This makes the total C2C incentives for *VC2* appreciably negative compared to other VCs as it will be getting that incentive.

7.3 Energy Trading With Consideration of Distribution Network Constraints

After modeling of the system in section 7.2, the distribution network constraints are incorporated in this section.

7.3.1 Problem Formulation

This section discusses the problem of the various elements involved in the system architecture.

7.3.1.1 System Architecture

In this work, all the buildings present on the same bus are gathered to form a virtual community (VC) (Figure7.8). A shareable battery energy storage system (BESS) is also considered in each VC, which is used to deal with the intermittent nature of renewable energy generation. The BESS also stores energy during low-price periods and discharge energy during high-price periods thereby reducing the dependency on the grid for energy demand. For facilitating the P2P energy exchange among building-to-building (B2B), building-to-community (B2C), and community-to-community (C2C), a secure and dedicated platform exists, specifically designed for limited information sharing and cloud computing. The primary objective behind employing the concept of VC is to alleviate the communication and computational stress that occurs in these P2P energy trading without jeopardizing any associated benefits. Also, this concept of VC allows for collective energy management and trading within the community itself. Each

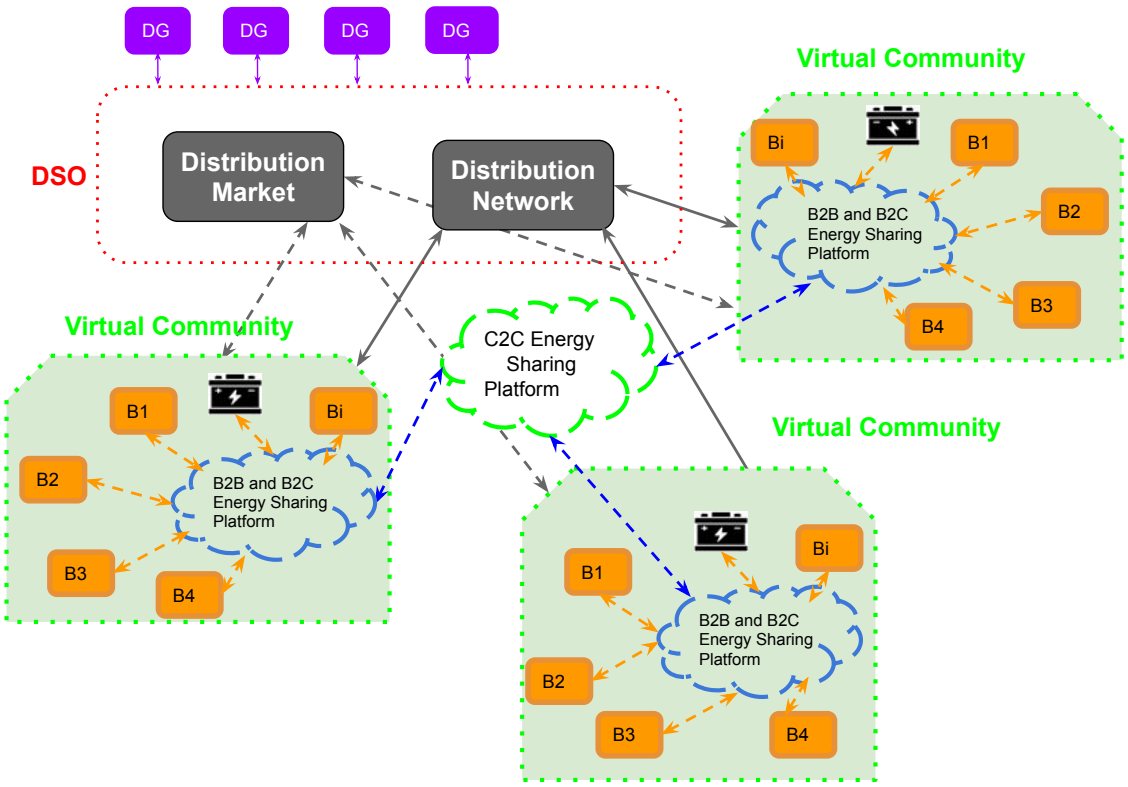

Figure 7.8: ILLUSTRATION OF PEER-TO-PEER LOCAL ENERGY TRADING

building is equipped with renewable energy generation modules. Buildings trade energy with other buildings and with the community in which it is present. The energy is aggregated with the help of VC which then trade with other VCs and with the grid. Thus, the buildings are not directly trading with the grid. Different DGs are also present, with the help of which the DSO maintains the grid parameters within their limits. The DSO is responsible for the entire network for ensuring stability by coordinating with all the network components, such as VCs and DGs, to manage energy flow and maintain the network parameters. A schematic view of the proposed work has been given in Figure 7.9, illustrating the various inputs and outputs, providing a brief insight as the system operations evolve from day-ahead to real-time.

7.3.1.2 Building Model

For i^{th} building of n^{th} community, the cost function can be expressed as

$$C^{B}_{n,i} = \sum_{t=1}^{T} C^{LS}_{n,i,t} + C^{b2b}_{n,i} + C^{b2c}_{n,i}, \tag{7.41}$$

where,

$$C^{LS}_{n,i,t} = \Lambda^{disc}_{t}(P^{LS}_{n,i,t} - L^{A}_{n,i,t})^2, \tag{7.42}$$

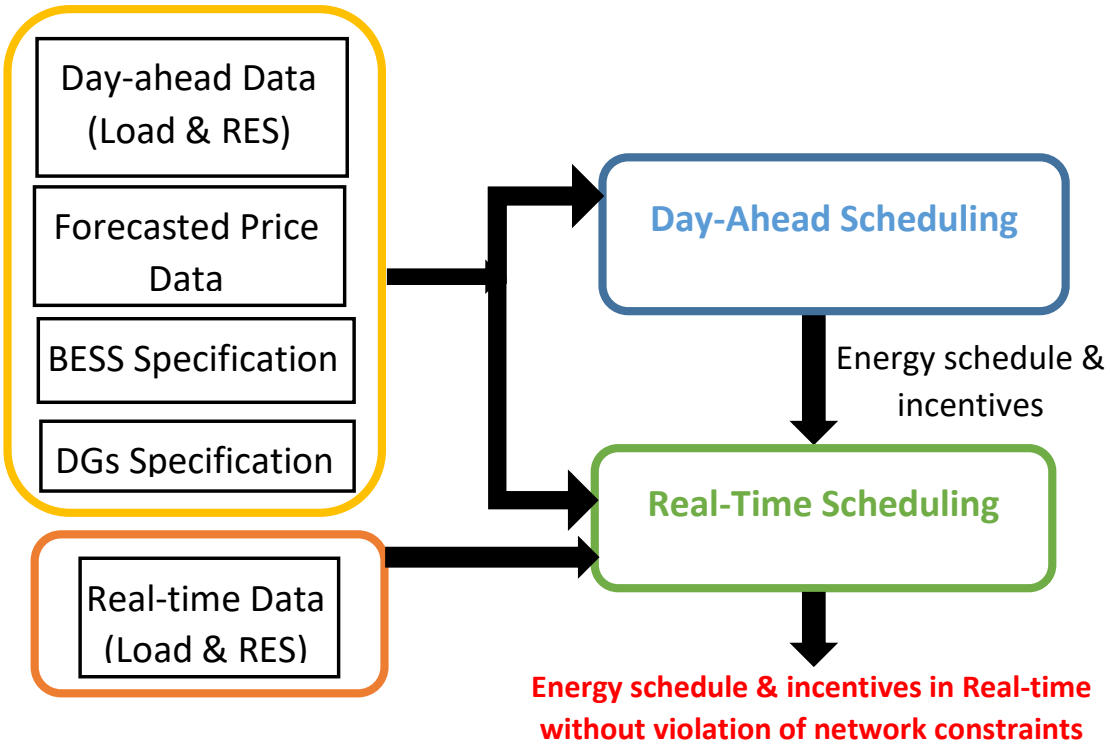

Figure 7.9: STRUCTURAL VIEW OF PROPOSED FRAMEWORK

$$C_{n,i}^{b2b} = \sum_{j=1,\ j\neq i}^{N_n^B} \pi_{n,i,j}^{b2b}, \quad \text{and} \tag{7.43}$$

$$C_{n,i}^{b2c} = \pi_{n,i}^{b2c}. \tag{7.44}$$

Here, $C_{n,i,t}^{LS}$, $C_{n,i}^{b2b}$, and $C_{n,i}^{b2c}$ represents the discomfort cost due to load shifting, energy trading cost in B2B, and that in B2C, respectively. And, Λ_t^{disc}, $P_{n,i,t}^{LS}$, and $L_{n,i,t}^{A}$ are the discomfort cost coefficient, load after shifting and load before shifting, respectively. In B2B trading, $P_{n,i,j,t}^{b2b}$, or B2C trading, $P_{n,i,t}^{b2c}$, the positive value signifies the power import, while the negative value indicates that power is exported from the building. Similarly, the positive values of incentives ($\pi_{n,i,j}^{b2b}$ and $\pi_{n,i}^{b2c}$) reveal that building is paying. The incentives are used to encourage the prosumers such that,

$$C_{n,i}^{B0} - C_{n,i}^{B} \geq 0. \tag{7.45}$$

Here, $C_{n,i}^{B0}$ is the cost of the building without P2P trading, where each building operates independently, purchasing electricity directly from the grid to meet the net load demand after using the renewable generations and demand responsive load. The other related constraints with respect to buildings are as follows.

$$L_{n,i,t}^{min} \leq P_{n,i,t}^{LS} \leq L_{n,i,t}^{max}, \tag{7.46}$$

$$\sum_{t=1}^{T} P_{n,i,t}^{LS} \geq \epsilon^{LS} \sum_{t=1}^{T} L_{n,i,t}^{A}. \tag{7.47}$$

$$P_{n,i,j,t}^{b2b} + P_{n,j,i,t}^{b2b} = 0, \qquad and \tag{7.48}$$

$$\pi_{n,i,j}^{b2b} + \pi_{n,j,i}^{b2b} = 0. \tag{7.49}$$

The equations (7.46) and (7.47) are associated with load shifting, i.e, maximum/minimum limit and load curtailment, respectively. The constraints (7.48) and (7.49) has variable of both i^{th} and j^{th} buildings of VC n. Thus, they are referred to as coupling constraints. For each building, the load should be balanced, and the respective load balancing equation can be given by

$$-\sum_{j=1,\ j\neq i}^{N_n^B} P_{n,i,j,t}^{b2b} - P_{n,i,t}^{b2c} = R_{n,i,t} - P_{n,i,t}^{LS}. \tag{7.50}$$

7.3.1.3 Virtual Community Model

For a virtual community (C_n^c), the cost function can be given by,

$$C_n^c = \sum_{t=1}^{T} (C_{n,t}^{U} + C_{n,t}^{BESS}) + C_n^{c2c}. \tag{7.51}$$

Here, $C_{n,t}^{U}$, $C_{n,t}^{BESS}$, and C_n^{c2c} comprises the total cost the VC has to pay. $C_{n,t}^{U}$ represents the cost involved in energy exchange with the utility. The battery utilization cost is given by $C_{n,t}^{BESS}$, and the cost that occurred due to energy exchange with other VCs is represented by C_n^{c2c}. These costs can be defined as follows.

$$C_{n,t}^{U} = (\Lambda_{n,t}^{im} + \epsilon^{CE}) P_{n,t}^{b} - \Lambda_{n,t}^{ex} P_{n,t}^{s}, \tag{7.52}$$

$$C_{n,t}^{BESS} = \Lambda^{UTI} (P_{n,t}^{ch} + P_{n,t}^{dis}), \quad \text{and} \tag{7.53}$$

$$C_n^{c2c} = \sum_{\substack{m=1 \\ m\neq n}}^{N^c} (\sum_{t=1}^{T} \Lambda_{n,m,t}^{NUC} P_{n,m,t}^{c2c} + \pi_{n,m}). \tag{7.54}$$

Here, $P_{n,t}^{s}$/ $P_{n,t}^{b}$, ϵ^{CE}, $\Lambda_{n,t}^{ex}$, and $\Lambda_{n,t}^{im}$ are the power exported/imported to/from the utility, charges due to carbon emission, power export price, and power import price respectively. $P_{n,t}^{ch}$ and $P_{n,t}^{dis}$ represents the charging and discharging power of BESS with Λ^{UTI} being its utilization coefficient. Inter-community power exchange ($P_{n,m,t}^{c2c}$) i.e. C2C power exchange, is treated as positive for import and negative for export. Similarly, the incentive ($\pi_{n,m}^{c2c}$) is considered to be

positive when the VC is paying else it will be negative. $\Lambda^{NUC}_{n,m,t}$ represents the dynamic network utilisation charge (NUC) and is given by the following equation.

$$\Lambda^{NUC}_{n,m,t} = \begin{cases} \frac{1}{2} max(\lambda^{LMP}_{t,n} - \lambda^{LMP}_{t,m}) & \text{if } P^{c2c}_{n,m,t} \geq 0 \text{ and } (\lambda^{LMP}_{t,n} - \lambda^{LMP}_{t,m}) \geq 0\,, \\ 0 & \text{if } P^{c2c}_{n,m,t} \geq 0 \text{ and } (\lambda^{LMP}_{t,n} - \lambda^{LMP}_{t,m}) < 0\,, \\ \frac{1}{2} max(\lambda^{LMP}_{t,m} - \lambda^{LMP}_{t,n}) & \text{if } P^{c2c}_{n,m,t} < 0 \text{ and } (\lambda^{LMP}_{t,m} - \lambda^{LMP}_{t,n}) \geq 0\,, \\ 0 & \text{if } P^{c2c}_{n,m,t} < 0 \text{ and } (\lambda^{LMP}_{t,m} - \lambda^{LMP}_{t,n}) < 0\,. \end{cases}$$

According to the above equation, the Network Utilization Charge (NUC) is applied when power is exported from a higher LMP bus to a lower LMP bus. The LMPs are determined using Optimal Power Flow (OPF), which considers voltage levels, line limits, and other relevant factors. If a peer-to-peer (P2P) energy exchange violates any system constraints, this is reflected in the LMP, leading to an increase in the NUC. The higher NUC then discourages excessive power exchange, prompting communities to adjust their exchanged power values. These updated values are subsequently used in the next OPF calculation. This iterative process continues until the difference between successive LMP values falls within an acceptable tolerance. In this way, the NUC helps manage line loading and voltage limits effectively.

Since the virtual community is identified as an unselfish structure in this work, the net cost of VC is divided into the buildings in the following way.

$$C^c_n = \sum_{i=1}^{N^B_n} \pi^{b2c}_{n,i}. \tag{7.55}$$

The constraints linked to the VC model are represented by the following equations.

$$SOC_{n,t} = (1 - \eta^{loss}_n) SOC_{n,t-1} + \eta^{ch}_n P^{ch}_{n,t} - \frac{1}{\eta^{dis}_n} P^{dis}_{n,t}\,, \tag{7.56}$$

$$P^{ch_{min}}_n \leq P^{ch}_{n,t} \leq P^{ch_{max}}_n, \tag{7.57}$$

$$P^{dis_{min}}_n \leq P^{dis}_{n,t} \leq P^{dis_{max}}_n, \tag{7.58}$$

$$SOC^{min}_n \leq SOC_{n,t} \leq SOC^{max}_n, \tag{7.59}$$

$$P^{c2c}_{n,m,t} + P^{c2c}_{m,n,t} = 0, \tag{7.60}$$

$$\pi^{c2c}_{n,m} + \pi^{c2c}_{m,n} = 0, \tag{7.61}$$

$$C^{c0}_n - C^c_n \geq 0, \qquad and \tag{7.62}$$

$$P^{b}_{n,t} - P^{s}_{n,t} + P^{dis}_{n,t} - P^{ch}_{n,t} + \sum_{\substack{m=1 \\ m \neq n}}^{N^C} P^{c2c}_{n,m,t} = \sum_{i=1}^{N^B_n} P^{b2c}_{n,i,t}. \tag{7.63}$$

The SOC level for the next stage is given by equation (7.56). The charging power, discharging power, and state of charge ($SoC_{n,t}$) are limited by equations (7.57), (7.58), and (7.59) respectively. The inter-community (C2C) energy exchange's constraints are given by equations (7.60) and (7.61). To motivate the VCs to take part in this C2C energy exchange, equation (7.62) is used. The C^{c0} in equation (7.62) is the cost that occurs to each VC when the C2C energy exchange does not exist. The equation (7.63) is used to ensure that the loads are balanced. The total number of VCs is equal to N^C and each VC n has N^B_n number of buildings. For each VC n, the net injection ($P^{net}_{n,t}$) is given by the algebraic sum of the net power exchanged with the utility and other VCs. This framework doesn't need any separate constraints to prevent simultaneous charging and discharging or buying and selling to the grid, as explained in Appendix III.

7.3.1.4 DGs

In the context of this proposed framework, the dispatchable DGs are assumed to be active and independent entities. Each DG provides its bid plan to the DSO. The objective function, C^{DG}_d, of d^{th} DG involves minimizing the generation cost while maximizing the revenue generated from supplying the distribution system and can be written as,

$$C^{DG}_d = \sum_{t=1}^{T} [c^a_d + c^b_d P^{DG}_{d,t} + c^c_d (P^{DG}_{d,t})^2 - \Lambda^{DG}_{d,t} P^{DG}_{d,t}], \tag{7.64}$$

$$s.t. \quad P^{min}_d \leq P^{DG}_{d,t} \leq P^{max}_d. \tag{7.65}$$

For d^{th} DG, the respective cost-attribute factors is given by c^a_d, c^b_d, & c^c_d. P^{min}_d & P^{max}_d are the limits of minimum and maximum power generation of d^{th} DG. $\Lambda^{DG}_{d,t}$ represents LMPs associated with the bus containing the d^{th} DG.

7.3.1.5 DSO

The DSO is obliged to maintain the network constraints. It is also accountable for local energy market clearance. It does so after acknowledging the load demand located at various buses. The DSO uses the optimum power flow to calculate the LMPs of different buses. The DSO demands $P^{DG'}_{d,t}$ from d^{th} DG at price $\Lambda^{DG}_{d,t}$ which is LMP associated with the bus containing that d^{th} DG.

Thus, for DSO, the cost function, C^{DSO}, can be written as,

$$C^{DSO} = \sum_{t=1}^{T}[\Lambda_t^{G,P} P_{1,t}^{G} + \Lambda_t^{G,Q} \left|Q_{1,t}^{G}\right| + \sum_{d=1}^{N_d}(\Lambda_{d,t}^{DG} P_{d,t}^{DG'})]. \tag{7.66}$$

The $\left|Q_{1,t}^{G}\right|$ can make the problem non-convex. So, instead of $\left|Q_{1,t}^{G}\right|$, in this framework $Q_{1,t}^{G^{aux}}$ is used in this framework such that $Q_{1,t}^{G^{aux}} \geq -Q_{1,t}^{G}$, $Q_{1,t}^{G^{aux}} \geq Q_{1,t}^{G}$ and $Q_{1,t}^{G^{aux}} \geq 0$. And the related constraints are given by,

$$\sum_{k=1}^{N^B} P_{k,t}^{G} - \sum_{k=1}^{N^B} P_{k,t}^{D} = 0 \quad : \lambda_t^1 \tag{7.67}$$

$$\sum_{k=1}^{N^B} Q_{k,t}^{G} - \sum_{k=1}^{N^B} Q_{k,t}^{D} = -\sum_{k'=1}^{N^B} b_{k'k'} \quad : \lambda_t^2 \tag{7.68}$$

During each time interval, to ensure the power balance in case of both active and reactive power, the constraints ((7.67),(7.68)) are used. The binary parameters $x_{k,d}^{DG}$, $x_{k,n}^{C}$, and x_k^{PCC} are used for representing the connection of DG, VC, and point of common coupling (PCC), respectively. The net active power generation ($P_{k,t}^{G}$) and demand ($P_{k,t}^{D}$), at bus k, are represented as follows.

$$P_{k,t}^{G} = x_k^{PCC} P_t^{G} + \sum_{d=1}^{N^{DG}} x_{k,d}^{DG} P_{d,t}^{DG'}, \qquad and \tag{7.69}$$

$$P_{k,t}^{D} = P_{k,t}^{FD} + \sum_{n=1}^{N^c} x_{k,n}^{C} P_{n,t}^{net'}. \tag{7.70}$$

For each VC n, the net injection ($P_{n,t}^{net'}$) is the algebraic total of net power exchanged with the utility and other VCs. The coupling constraints for VC, DG, and DSO models are $P_{n,t}^{net'} = P_{n,t}^{net}$ and $P_{d,t}^{DG'} = P_{d,t}^{DG}$. Similarly, for all the buses, the overall reactive power demand and generation can be represented.

$$-P_l^{max} \leq \sum_{k=1}^{N^B} f_{l-k}^{P-P}(P_{k,t}^{G} - P_{k,t}^{D}) + \sum_{k=1}^{N^B} f_{l-k}^{P-Q}(Q_{k,t}^{G} - Q_{k,t}^{D}) \leq P_l^{max} \quad : \mu_{l,t}^1, \mu_{l,t}^2 \quad \forall l \tag{7.71}$$

$$V^{min} \leq \sum_{k=1}^{N^B} X_{N^B+k',k}(P_{k,t}^{G} - P_{k,t}^{D}) + \sum_{k=1}^{N^B} X_{N^B+k',N^B+k}(Q_{k,t}^{G} - Q_{k,t}^{D}) \leq V^{max} : \mu_{k',t}^3,\ \mu_{k',t}^4\ \forall k' \tag{7.72}$$

$$P^G_{min} \leq P^G_t \leq P^G_{max} : \mu^5_t, \mu^6_t \tag{7.73}$$

$$Q^G_{min} \leq Q^G_t \leq Q^G_{max} : \mu^7_t, \mu^8_t \tag{7.74}$$

The constraint (7.71) refers to the line flow limit consisting of factors (f^{P-P}_{l-k} and f^{P-Q}_{l-k}) that are known as generation shift distribution (GSD) factors. These factors have been discussed in Appendix I and are derived from [81]. The constraint (7.72) is used to make sure that the voltage at each bus doesn't violate its limit. The term $X_{k,k'}$ is related to the network topology and is described in the network topology. The constraint related to active and reactive power exchange at the point of common coupling is given by the equations (7.73) and (7.74). The Lagrangian function for the DSO is formed with the help of its objective and constraints to calculate the various LMPs. In the context of this research, it is presumed that negligible reactive power is exchanged by the VC with the distribution network. Hence, this problem formulation only considers LMPs related to active power. Therefore, at k^{th} bus, the active power LMP is derived by partially differentiating the Lagrangian function with respect to the net power demanded at that bus. Thus, the active power LMP is represented as follows.

$$\lambda^{LMP}_{t,k} = \lambda^1_t + \sum_l (-\mu^1_{l,t} + \mu^2_{l,t}) f^{P-P}_{l-k} + \sum_{k'} (-\mu^3_{k',t} + \mu^4_{k',t}) X_{N^B+k',k}. \tag{7.75}$$

7.3.2 Research Methodology

The research methodology is further divided into two sections to explain the day-ahead and real-time model.

7.3.2.1 Day Ahead Model

The cooperative game theory is used in this work to manage the energy trade among buildings and virtual communities. Hong's 2p point estimate method (PEM) [77] is used for dealing with the uncertainties concerning the RESs as described in Section 2.9. In subsequent sections, only the cost function is denoted by $\mathbb{E}(.)$ instead of all variables for simplicity.

A modified Nash bargaining problem (MNBP) is used for obtaining the Nash equilibrium for the system discussed in section 7.3.1. This modified version is Kalai–Smorodinsky (KS) bargaining solution [84]. Thus, the modified cooperative game can be described as given in Table 7.4. The game is played in two levels due to the presence of B2C coupled variables.

Table 7.4: DESCRIPTION OF THE COOPERATIVE GAME

Levels	Players	Strategies	Objectives
1	Buildings	$X^{B}_{n,i,t}$:=($P^{LS}_{n,i,t}$, $P^{b2b}_{n,i,j,t}$, $P^{b2c}_{n,i,t}$, $\pi^{b2b}_{n,i,j}$, $\pi^{b2c}_{n,i}$)	$C^{b}_{n,i}$
2	VCs	$X^{c}_{n,t}$:= ($P^{b}_{n,t}$, $P^{s}_{n,t}$, $P^{ch}_{n,t}$, $P^{dis}_{n,t}$, $P^{c2c}_{n,m,t}$, $\pi^{c2c}_{n,m}$)	C^{c}_{n}

And the required problem becomes as follows.

$$\mathscr{F}_1 : \ max\Bigg[\prod_{n=1}^{N^C}\Bigg\{\prod_{i=1}^{N^B_n}\Bigg(\mathbb{E}(C^{B0}_{n,i}) - \mathbb{E}(C^{B}_{n,i})\Bigg)(\mathbb{E}(C^{c0}_{n}) - \mathbb{E}(C^{c}_{n}))\Bigg\}\Bigg]. \tag{7.76}$$

subject to:

$$\mathbb{E}(C^{B0}_{n,i}) - \mathbb{E}(C^{B}_{n,i}) = K^{b2b}_{n,i}(\mathbb{E}(C^{B0}_{n,i}) - \mathbb{E}(C^{B*}_{n,i})), \tag{7.77}$$

$$\mathbb{E}(C^{c0}_{n}) - \mathbb{E}(C^{c}_{n}) = K^{c2c}_{n}(\mathbb{E}(C^{c0}_{n}) - \mathbb{E}(C^{c*}_{n})), \tag{7.78}$$

$$K^{b2b}_{n,i} = K^{b2b}_{n,j}, \quad j = 1, 2....N^B_n \tag{7.79}$$

$$K^{c2c}_{n} = K^{c2c}_{m}, \quad m = 1, 2....N^C. \tag{7.80}$$

Here the expected cost in the best case is represented by $\mathbb{E}(C^{B*}_{n,i})$ and $\mathbb{E}(C^{c*}_{n})$. In this work, the best case is assumed to be that case where the energy transacted with peers is purchased/sold at the same rate as that of transacting energy to/from the utility, respectively. The variables $K^{b2b}_{n,i}$ and K^{c2c}_{n} are used to ensure a fair incentive distribution such that the ratio of optimal cost reduction and best cost reduction is the same for each peer. Therefore, $K^{b2b}_{n,i}$ and K^{c2c}_{n} will also be included in the courses of action of buildings and VCs. Based on the results of the preceding iteration, $C^{B*}_{n,i}$ and C^{c*}_{n} are calculated for each iteration, and therefore they become a fixed parameter for the current iteration. The reason behind this is to preserve the convex characteristic of the objective functions. The maximization problem of equation (7.76) is transformed into a minimization problem in the following manner.

$$\mathscr{F}_2 : \ min\Bigg[-\sum_{n=1}^{N^C}\Bigg\{\sum_{i=1}^{N^B_n} log\Bigg(1 + \mathbb{E}(C^{B0}_{n,i}) - \mathbb{E}(C^{B}_{n,i})\Bigg) + log\Bigg(1 + \mathbb{E}(C^{c0}_{n}) - \mathbb{E}(C^{c}_{n})\Bigg)\Bigg\}\Bigg]. \tag{7.81}$$

The problem (7.81) can be solved in a decentralized way using the alternating direction method of multipliers (ADMM) [76] by decoupling the coupling constraints:{(7.48),

(7.49), (7.60), (7.61), (7.63), (4.23), (7.79), and (7.80)$\}$. This requires the auxiliary variables ($\sigma_{n,i,j,t}^{P_{b2b}}, \sigma_{n,i,j}^{\pi_{b2b}}, \sigma_{n,m,t}^{P_{c2c}}, \sigma_{n,m}^{\pi_{c2c}}, \sigma_{n,i,t}^{P_{b2c}}, \sigma_{n,i}^{\pi_{b2c}}, \sigma_{n,i}^{K^{b2b}}$ and $\sigma_{n}^{K^{c2c}}$) employed for $P_{n,i,j,t}^{b2b}$, $\pi_{n,i,j}^{b2b}$, $P_{n,m,t}^{c2c}$, $\pi_{n,m}^{c2c}$, $P_{n,i,t}^{b2c}$, $\pi_{n,i}^{b2c}$, $K_{n,i}^{b2b}$, and K_{n}^{c2c}, respectively. Therefore, the reformulated coupling constraints are as follows.

$$\sigma_{n,i,j,t}^{P_{b2b}} + \sigma_{n,j,i,t}^{P_{b2b}} = 0, \tag{7.82}$$

$$\sigma_{n,i,j}^{\pi_{b2b}} + \sigma_{n,j,i}^{\pi_{b2b}} = 0, \tag{7.83}$$

$$\sigma_{n,m,t}^{P_{c2c}} + \sigma_{m,n,t}^{P_{c2c}} = 0, \tag{7.84}$$

$$\sigma_{n,m}^{\pi_{c2c}} + \sigma_{m,n}^{\pi_{c2c}} = 0, \tag{7.85}$$

$$\sigma_{n,i}^{K^{b2b}} = \sigma_{n,j}^{K^{b2b}}, \quad j = 1, 2....N_n^B \tag{7.86}$$

$$\sigma_{n}^{K^{c2c}} = \sigma_{m}^{K^{c2c}} \quad m = 1, 2....N^C \tag{7.87}$$

$$P_{n,t}^{b} - P_{n,t}^{s} + P_{n,t}^{dis} - P_{n,t}^{ch} + \sum_{\substack{m=1 \\ m \neq n}}^{N^C} P_{n,m,t}^{c2c} = \sum_{i=1}^{N_n^B} \sigma_{n,i,t}^{P_{b2c}}, \qquad and \tag{7.88}$$

$$C_n^c = \sum_{i=1}^{N_n^B} \sigma_{n,i}^{\pi_{b2c}}. \tag{7.89}$$

The equation (7.81) can be restructured as per these decoupled constraints in the following manner.

$$\mathscr{F}_3: \ min\Bigg[\Bigg[-\sum_{n=1}^{N^C}\Bigg\{\sum_{i=1}^{N_n^B} log(1+\mathbb{E}(C_{n,i}^{B0})-\mathbb{E}(C_{n,i}^{B})) + log(1+\mathbb{E}(C_n^{c0})-\mathbb{E}(C_n^c))\Bigg\}\Bigg] + \sum_{n=1}^{N^C}\sum_{i=1}^{N_n^B}\Bigg[\sum_{\substack{j=1\\ j\neq i}}^{N_n^B}\Bigg\{\sum_{t=1}^{T}\frac{\delta_1}{2}(P_{n,i,j,t}^{b2b} - \sigma_{n,i,j,t}^{P_{b2b}} + \frac{\omega_{n,i,j,t}^{P_{b2b}}}{\delta_1})^2 + \frac{\delta_2}{2}(\pi_{n,i,j}^{b2b} - \sigma_{n,i,j}^{\pi_{b2b}} + \frac{\omega_{n,i,j}^{\pi_{b2b}}}{\delta_2})^2\Bigg\} + \frac{\delta_{12}}{2}(K_{n,i}^{b2b} - \sigma_{n,i}^{K^{b2b}} + \frac{\omega_{n,i}^{K^{b2b}}}{\delta_{12}})^2\Bigg] + \sum_{n=1}^{N^C}\sum_{i=1}^{N_n^B}\Bigg[\sum_{t=1}^{T}\frac{\delta_3}{2}(P_{n,i,t}^{b2c} - \sigma_{n,i,t}^{P_{b2c}} + \frac{\omega_{n,i,t}^{P_{b2c}}}{\delta_3})^2 + \frac{\delta_4}{2}(\pi_{n,i}^{b2c} - \sigma_{n,i}^{\pi_{b2c}} + \frac{\omega_{n,i}^{\pi_{b2c}}}{\delta_4})^2\Bigg] + \sum_{n=1}^{N^C}\Bigg[\sum_{\substack{m=1\\ m\neq n}}^{N^C}\Bigg\{\sum_{t=1}^{T}\frac{\delta_5}{2}(P_{n,m,t}^{c2c} - \sigma_{n,m,t}^{P_{c2c}} + \frac{\omega_{n,m,t}^{P_{c2c}}}{\delta_5})^2 + \frac{\delta_6}{2}(\pi_{n,m}^{c2c} - \sigma_{n,m}^{\pi_{c2c}} + \frac{\omega_{n,m}^{\pi_{c2c}}}{\delta_6})^2\Bigg\} + \frac{\delta_{56}}{2}(K_n^{c2c} - \sigma_n^{K^{c2c}} + \frac{\omega_n^{K^{c2c}}}{\delta_{56}})^2\Bigg]\Bigg]. \quad (7.90)$$

The ω, σ, and δ are dual multipliers, auxiliary variables, and penalty parameters, respectively. The variables for the above problem are X^B, X^c, and σ; And the constraints are γ_B :=[(7.46) to (7.45), (7.50),(7.77)], γ_c :=[$P^B \geq 0$, $P^s \geq 0$, (7.57) to (7.59), (7.62), (7.88),(7.89),(7.78)], γ_1 :=[(7.82), (7.83),(7.86)], and γ_2 :=[(7.84), (7.85),(7.87)].

The complete model for day-ahead market clearing considering network constraints and all participants' problems is given by the following equations.

$$\mathscr{F}'_2: \ min\Bigg[-\sum_{n=1}^{N^C}\{\sum_{i=1}^{N_n^B} log\left(1+\mathbb{E}(C_{n,i}^{B0})-\mathbb{E}(C_{n,i}^{B})\right) + log\left(1+\mathbb{E}(C_n^{c0})-\mathbb{E}(C_n^c)\right)\} + \sum_{d=1}^{N^{DG}} C_d^{DG} + C^{DSO}\Bigg]. \quad (7.91)$$

Along with the coupling constraints mentioned above, the net power injection and DG's power in the day ahead model is given to the DSO in a decentralised way, resulting in the following

model.

$$\mathscr{F}'_3 : \ min\Bigg[[-\sum_{n=1}^{N^C}\{\sum_{i=1}^{N_n^B} log(1+\mathbb{E}(C_{n,i}^{B0})-\mathbb{E}(C_{n,i}^{B}))$$
$$+ log(1+\mathbb{E}(C_n^{c0})-\mathbb{E}(C_n^{c}))\}]+\sum_{n=1}^{N^C}\sum_{i=1}^{N_n^B}[\sum_{\substack{j=1\\ j\neq i}}^{N_n^B}\{\sum_{t=1}^{T}\frac{\delta_1}{2}(P_{n,i,j,t}^{b2b}$$
$$-\sigma_{n,i,j,t}^{P_{b2b}}+\frac{\omega_{n,i,j,t}^{P_{b2b}}}{\delta_1})^2+\frac{\delta_2}{2}(\pi_{n,i,j}^{b2b}-\sigma_{n,i,j}^{\pi_{b2b}}+\frac{\omega_{n,i,j}^{\pi_{b2b}}}{\delta_2})^2\}+$$
$$\frac{\delta_{12}}{2}(K_{n,i}^{b2b}-\sigma_{n,i}^{K^{b2b}}+\frac{\omega_{n,i}^{K^{b2b}}}{\delta_{12}})^2]+\sum_{n=1}^{N^C}\sum_{i=1}^{N_n^B}[\sum_{t=1}^{T}\frac{\delta_3}{2}(P_{n,i,t}^{b2c}-$$
$$\sigma_{n,i,t}^{P_{b2c}}+\frac{\omega_{n,i,t}^{P_{b2c}}}{\delta_3})^2+\frac{\delta_4}{2}(\pi_{n,i}^{b2c}-\sigma_{n,i}^{\pi_{b2c}}+\frac{\omega_{n,i}^{\pi_{b2c}}}{\delta_4})^2]+$$
$$\sum_{n=1}^{N^C}[\sum_{\substack{m=1\\ m\neq n}}^{N^C}\{\sum_{t=1}^{T}\frac{\delta_5}{2}(P_{n,m,t}^{c2c}-\sigma_{n,m,t}^{P_{c2c}}+\frac{\omega_{n,m,t}^{P_{c2c}}}{\delta_5})^2+\frac{\delta_6}{2}(\pi_{n,m}^{c2c}-$$
$$\sigma_{n,m}^{\pi_{c2c}}+\frac{\omega_{n,m}^{\pi_{c2c}}}{\delta_6})^2\}+\frac{\delta_{56}}{2}(K_n^{c2c}-\sigma_n^{K^{c2c}}+\frac{\omega_n^{K^{c2c}}}{\delta_{56}})^2]+$$
$$\sum_{d=1}^{N^{DG}}C_d^{DG}+C^{DSO}+\sum_{n=1}^{N^C}\{\sum_{t=1}^{T}\frac{\delta_7}{2}(P_{n,t}^{net}-P_{n,t}^{net'}+\frac{\omega_{n,t}^{P^{net}}}{\delta_7})^2\}+$$
$$\sum_{d=1}^{N^{DG}}\{\sum_{t=1}^{T}\frac{\delta_7}{2}(P_{d,t}^{DG}-P_{d,t}^{DG'}+\frac{\omega_{d,t}^{P^{DG}}}{\delta_7})^2\}\Bigg]. \quad (7.92)$$

The flowchart shown in Figure 7.10 represents this decentralized energy scheduling completely. The primal residual ($\lambda^P = ||X(\kappa+1)-\sigma(\kappa+1)||$) and dual residual ($\lambda^D = ||\sigma(\kappa+1)-\sigma(\kappa)||$) are used for updating ω and δ. Therefore, ω and δ get updated in the following way.

$$\omega(\kappa+1)=\omega(\kappa)+\delta(\kappa)(X(\kappa+1)-\sigma(\kappa+1)), \quad (7.93)$$

$$\delta(\kappa+1)=\begin{cases}\frac{\delta(\kappa)}{\nu}, & \text{if } \lambda^P<\tau\lambda^D,\\ \nu\delta(\kappa), & \text{if } \lambda^P>\frac{\lambda^D}{\tau},\\ \delta(\kappa), & \text{otherwise.}\end{cases} \quad (7.94)$$

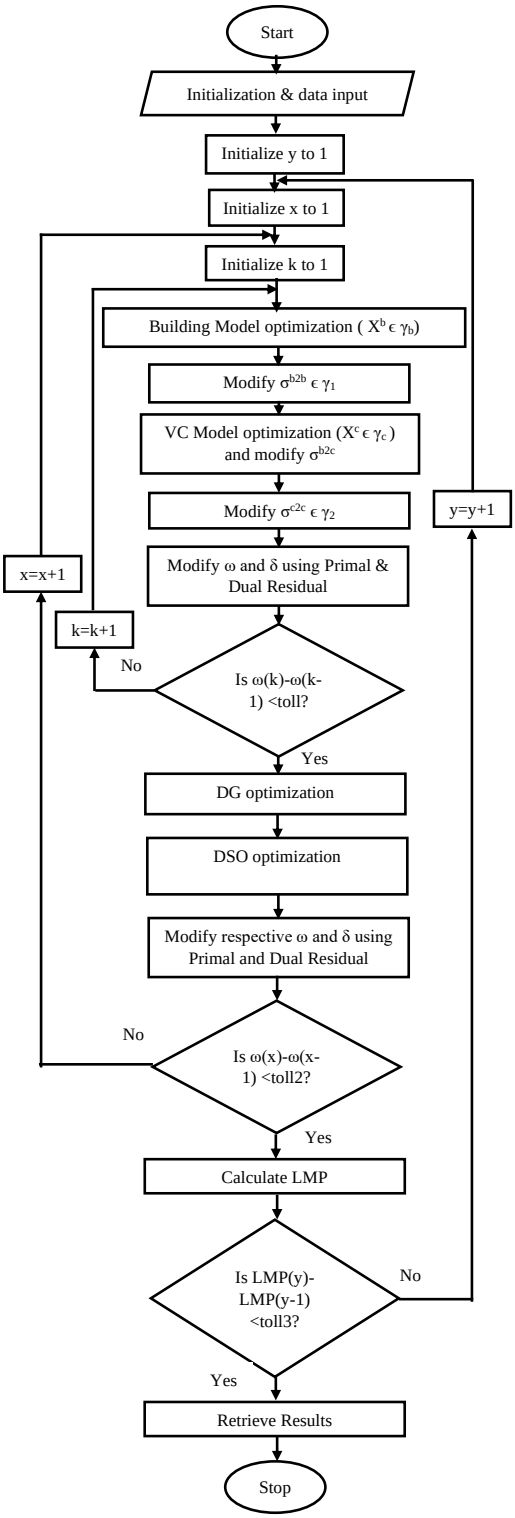

Figure 7.10: FLOWCHART FOR DAY-AHEAD P2P ENERGY TRADING

7.3.2.2 Real Time Market

Based on the day-ahead market commitments, the real-time market is executed. The B2B and C2C power and incentive from the day-ahead market are considered as fixed parameters for the real-time market. Along with that, the LMP from the day ahead market is also used in this model. The whole process for the real-time market is described briefly in the flowchart shown in Figure 7.11.

7.3.2.2.1 VC-Building Energy Trade The above model will work similarly to that described in section 7.3.2.1 with B2B and C2C related parameters fixed. The net injection in the real-time model will be directly transferred to the DSO. However, since this model works in real-time, there will be issues in managing BESS for each hour. To solve this problem, the receding horizon method [79] is incorporated into this real-time model. For each hour, as shown in Figure 7.11, the problem will be solved repeatedly by making the variable of the previous hour constant to the value assigned to them in that previous hour. The data required for future hours will be taken from the day-ahead model. The net injection will be given directly to the DSO for each hour.

7.3.2.2.2 DG-DSO Energy Trade For each hour, the DSO will optimize using the Day-ahead value of DG power and the net injection of each community for that particular hour as shown in Figure 7.11. In case the DSO model becomes infeasible, then for that hour, a pseudo-DSO model will run for each hour whose objective will be,

$$C_t^{DSO^{pseudo}} = [\Lambda_t^{G,P} P_t^{G^{rt}} + \Lambda_t^{G,Q} \left| Q_t^{G^{rt}} \right| + \sum_{d=1}^{N_d} (\Lambda_{d,t}^{DG} P_{d,t}^{DG'})]. \tag{7.95}$$

Here $P_{d,t}^{DG'}$ is the DG power offered in the pseudo case, and it is compared from the day ahead value, $P_{d,t}^{DG}$, for the increment and increment of the bidding prices.

$$P_{d,t}^{DG'^{rt}_{in}} = \begin{cases} P_{d,t}^{DG'} - P_{d,t}^{DG}, & \text{if } P_{d,t}^{DG'} - P_{d,t}^{DG} > 0, \\ 0, & \text{otherwise.} \end{cases} \tag{7.96}$$

$$P_{d,t}^{DG'^{rt}_{dc}} = \begin{cases} P_{d,t}^{DG} - P_{d,t}^{DG'}, & \text{if } P_{d,t}^{DG} - P_{d,t}^{DG'} > 0, \\ 0, & \text{otherwise.} \end{cases} \tag{7.97}$$

Here $P_{d,t}^{DG'^{rt}_{in}}$ is the increase in the DG power from the day ahead value $P_{d,t}^{DG}$ and $P_{d,t}^{DG'^{rt}_{dc}}$ is the decrease in the DG power from the day ahead value, $P_{d,t}^{DG}$. Also, $P_{d,t}^{DG'^{rt}_{in}}$ and$P_{d,t}^{DG'^{rt}_{dc}}$ both are

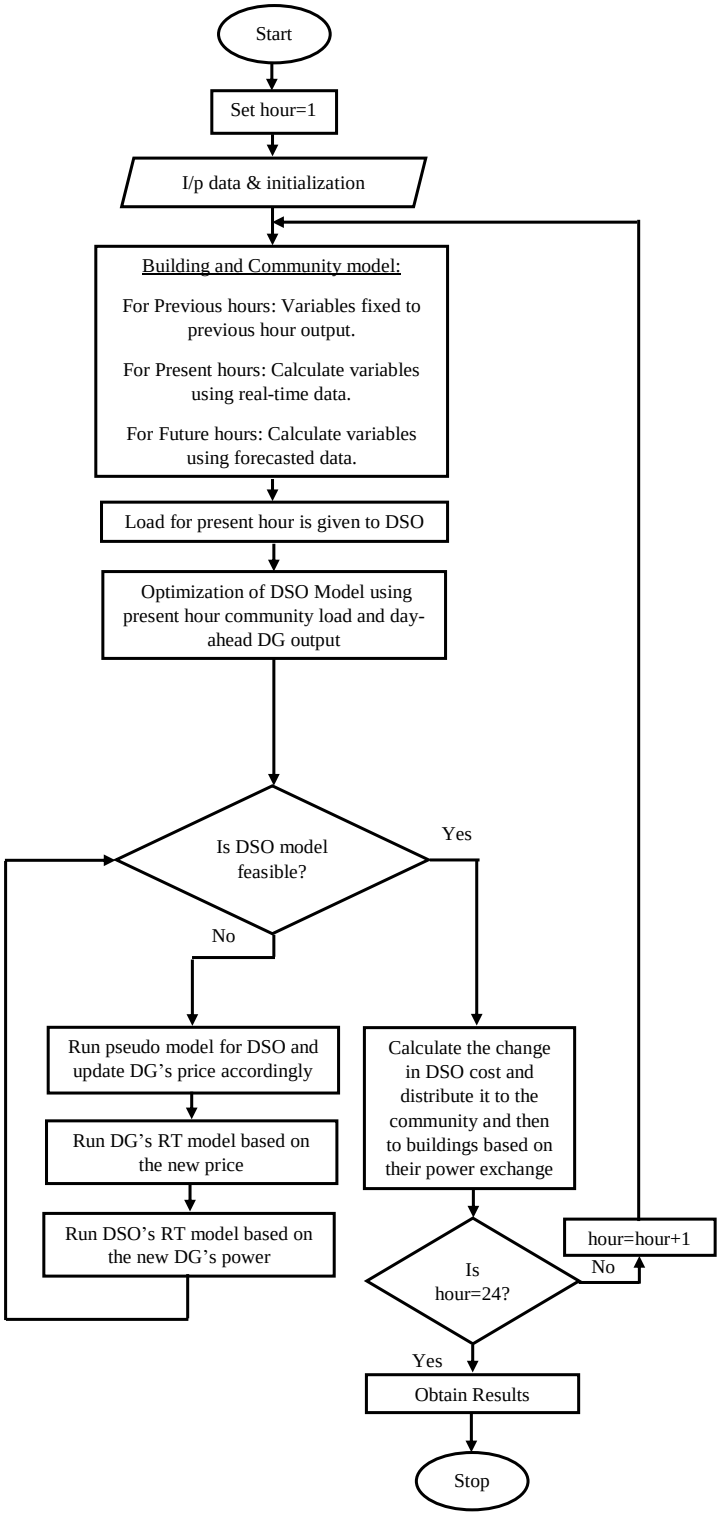

Figure 7.11: FLOWCHART FOR REAL-TIME MODEL

DSO's variable. Here $\Lambda_{d,t}^{DG}$ is the day-ahead LMP. Depending on $P_{d,t}^{DG'^{rt}_{in}}$ and $P_{d,t}^{DG'^{rt}_{dc}}$, the value of $\Lambda_{d,t}^{DG^{rt}_{in}}$ and $\Lambda_{d,t}^{DG^{rt}_{dc}}$ changes as follows.

$$\Lambda_{d,t}^{DG^{rt}_{in}} = \begin{cases} \Lambda_{d,t}^{DG^{rt}_{in}} + 0.001, & \text{if } P_{d,t}^{DG'^{rt}_{in}} > 0, \\ \Lambda_{d,t}^{DG^{rt}_{in}}, & \text{otherwise.} \end{cases} \tag{7.98}$$

$$\Lambda_{d,t}^{DG^{rt}_{dc}} = \begin{cases} \Lambda_{d,t}^{DG^{rt}_{dc}} + 0.001, & \text{if } P_{d,t}^{DG'^{rt}_{dc}} > 0, \\ \Lambda_{d,t}^{DG^{rt}_{dc}}, & \text{otherwise.} \end{cases} \tag{7.99}$$

The initial value of $\Lambda_{d,t}^{DG^{rt}_{in}}$ is $\Lambda_{d,t}^{DG}$ and $\Lambda_{d,t}^{DG^{rt}_{dc}}$ is zero. This increment process is continued until the DSO model becomes feasible. The DSO model is represented by

$$C_t^{DSO^{rt}} = \Lambda_t^{G,P} P_t^{G^{rt}} + \Lambda_t^{G,Q} \left| Q_t^{G^{rt}} \right| + \sum_{d=1}^{N_d} [\Lambda_{d,t}^{DG}(P_{d,t}^{DG} - P_{d,t}^{DG^{rt}_{dc}}) + \Lambda_{d,t}^{DG^{rt}_{in}} P_{d,t}^{DG^{rt}_{in}} + \Lambda_{d,t}^{DG^{rt}_{dc}} P_{d,t}^{DG^{rt}_{dc}}]. \tag{7.100}$$

The constraints are the same in the day-ahead model except for the load balancing equations (7.69,7.70), which will change accordingly. In equation (7.100), $P_{d,t}^{DG^{rt}_{in}}$ and $P_{d,t}^{DG^{rt}_{dc}}$ are given by DG using following model.

$$C_{d,t}^{DG^{rt}} = c_d^a + c_d^b P_{d,t}^{DG^{rt}} + c_d^c (P_{d,t}^{DG^{rt}})^2 - \Lambda_{d,t}^{DG}(P_{d,t}^{DG^{rt}} - P_{d,t}^{DG^{rt}_{in}}) - \Lambda_{d,t}^{DG^{rt}_{in}} P_{d,t}^{DG^{rt}_{in}} - \Lambda_{d,t}^{DG^{rt}_{dc}} P_{d,t}^{DG^{rt}_{dc}}, \tag{7.101}$$

subjected to

$$P_d^{min} \leq P_{d,t}^{DG^{rt}} \leq P_d^{max}, \tag{7.102}$$

$$P_{d,t}^{DG^{rt}_{dc}} \leq (P_{d,t}^{DG} - P_{d,t}^{DG^{rt}}) - \kappa_{d,t} P_{d,t}^{DG} + P_{d,t}^{DG_{aux}}, \tag{7.103}$$

$$P_{d,t}^{DG^{rt}_{in}} \leq P_{d,t}^{DG_{aux}} - \kappa_{d,t} P_{d,t}^{DG}, \tag{7.104}$$

where $P_{d,t}^{DG^{rt}_{dc}} \geq 0$, $P_{d,t}^{DG^{rt}_{in}} \geq 0$, $P_{d,t}^{DG_{aux}} \geq 0$, and $P_{d,t}^{DG_{aux}}$ is an auxiliary variable such that,

$$P_{d,t}^{DG_{aux}} \leq P_{d,t}^{DG^{rt}}, \tag{7.105}$$

$$P_{d,t}^{DG_{aux}} \geq P_{d,t}^{DG^{rt}} - (1 - \kappa_{d,t})M, \quad \text{and} \tag{7.106}$$

$$P_{d,t}^{DG_{aux}} \leq \kappa_{d,t} M. \tag{7.107}$$

Here, M is assumed to be a very large number, and $\kappa_{d,t}$ is a binary variable. The change in DSO's cost function is divided into community and further buildings based on their power exchange.

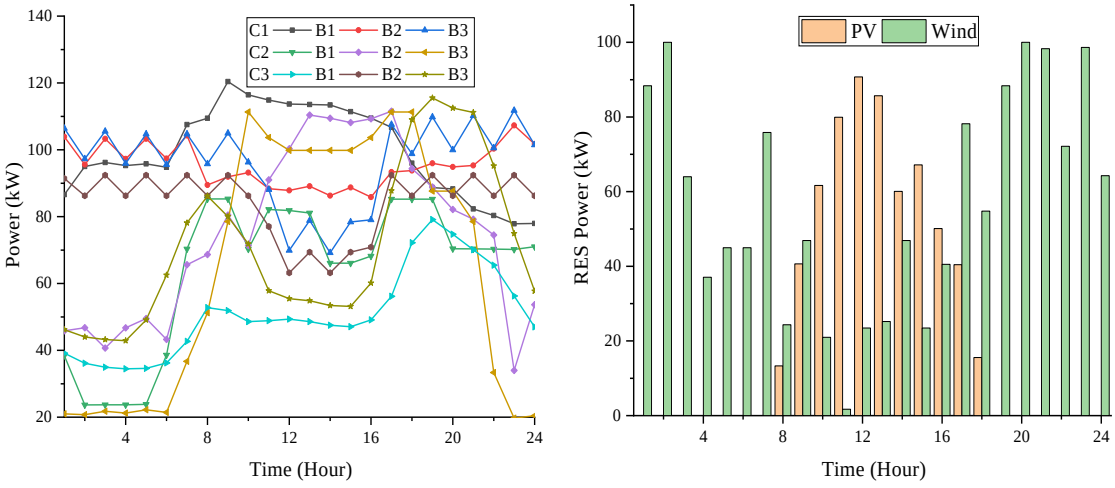

(a) (b)

Figure 7.12: (A) LOAD DEMAND CURVES OF BUILDINGS (B) RES POWER GENERATION

7.3.3 Simulation Results

In the context of this work, the IEEE 33 bus system with two DGs and nine buildings (B_i) equipped with RESs generations (Figure 7.12(b)) are considered as given in Appendix II. Each building has different load curves (Figure 7.12(a)), and the buildings present on the same bus are aggregated under VC. In this work, three VCs (*VC1*, *VC2*, and *VC3*) are considered, which are located at buses 21, 24, and 18, respectively. The capacity rating of Wind power generation (WPG) and solar power generation (SPG) in Figure 7.12(b) is 100kW and 125kW, respectively. All the buildings have the installed capacity of SG and WG as 100 kW and 50 kW/h, respectively, except for the building in *VC1*, and B_2 & B_3 in *VC2* that have the same capacity as shown in Figure 7.12(b). The power limit for charging/discharging of the community BESS (rated 200 kW) is 50 kW/h. These BESS have SOC limits of [20%,90%]. Up to $\pm 10\%$, the shifting of the load is permitted with the fraction of load supplied, ϵ_{LS}, equals to one. Other related parameters are mentioned in the Table 7.2. The price when power is imported from the utility is shown in Figure 7.15(a). The respective power export price is presumed to be in a constant proportion to that of power import. The DGs are present on buses 6 and 13. And the related parameters ($c_d^a, c_d^b, c_d^c, P_d^{min}, P_d^{max}$) of these two DGs are given by (0\$, $0.24\$/kW$, $0.0020\$/kW^2$, $0kW$, $2000kW$) and (0\$, $0.24\$/kW$, $0.0025\$/kW^2$, $0kW$, $2000kW$) respectively. For optimization, the GAMS/CONOPT4 and CPLEX solver is used on a laptop with configuration of 8 GB RAM and a Core $i3$ 1.20 GHz processor.

The following cases have been examined to demonstrate the effectiveness of the proposed framework.

Case I (Base or Reference case): This shows the complete non-existence of P2P energy trading. Here, all the buildings solely engage with the utility for energy exchange. Apart from being the benchmark case, this case highlights the limitations in local energy management in the absence of prosumer interactions.

Case II: The existence of P2P energy exchange is assumed in this case, with only buildings engaging in energy exchange among themselves (B2B) and its VC (B2C), each equipped with a shareable BESS. The buildings exchange energy with the utility through VCs, who are responsible for trading with the utility. For a particular hour, the role of buildings grouped under a VC, as a buyer or seller in B2B energy trading, is determined endogenously by the buildings based on their excess energy and their net cost saving. The BESS helps in balancing the supply and demand within a VC and deals with the uncertainties arising from renewable energy generations. The VCs are responsible for communicating with the utility and showing decentralised control's effectiveness.

Case III: Moreover, in conjunction with the case mentioned above (*Case II*), C2C energy exchange is also present in this case. The role of VCs is extended from interacting with the utility only to interacting with other VCs. The interaction among VCs maximizes the benefits due to the enhanced load diversity across the network. Similar to (*Case II*), for a particular hour, VCs' role as buyers or sellers in C2C energy trading is determined endogenously by the VCs based on their excess energy and net cost saving. The formation of VCs and their interaction makes it easy for the DSO to control the network parameters with the help of dynamic network usage charges applied with each C2C energy trade.

Real-time case: Based on the day ahead scheduling results (*Case III*), the real-time energy market is operated and the results are illustrated. The BESS is used in real-time energy market and the network constraints are maintained with the help of DGs by DSO as discussed in section III-B.

The above first three cases, without considering the network constraints, have been investigated in the earlier section 7.2. The *Case III** refers to the *Case III* of section 7.2 where the network constraints were ignored. The primary P2P simulation-based results have been covered in section 7.2. Here, the effect of the integration of grid constraints and implementation in real-time is discussed.

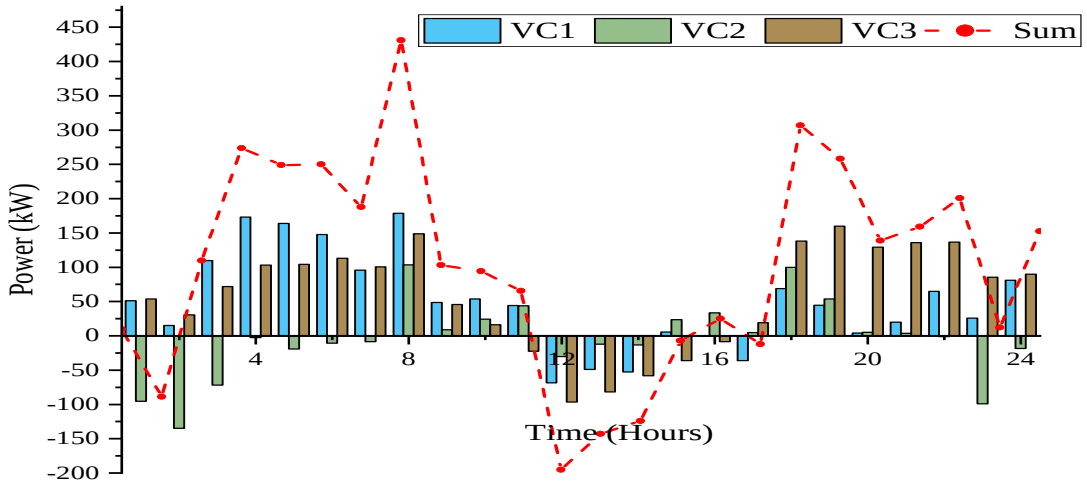

(a)

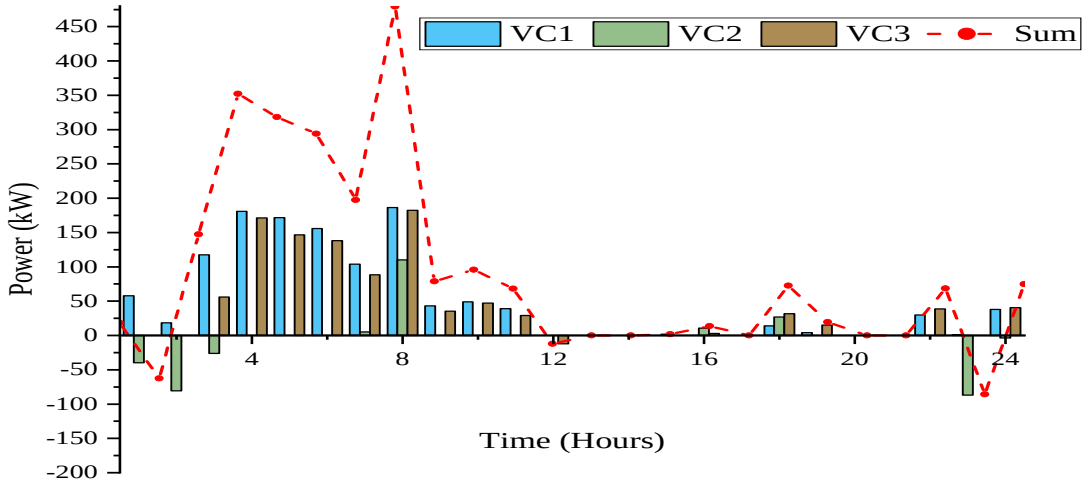

(b)

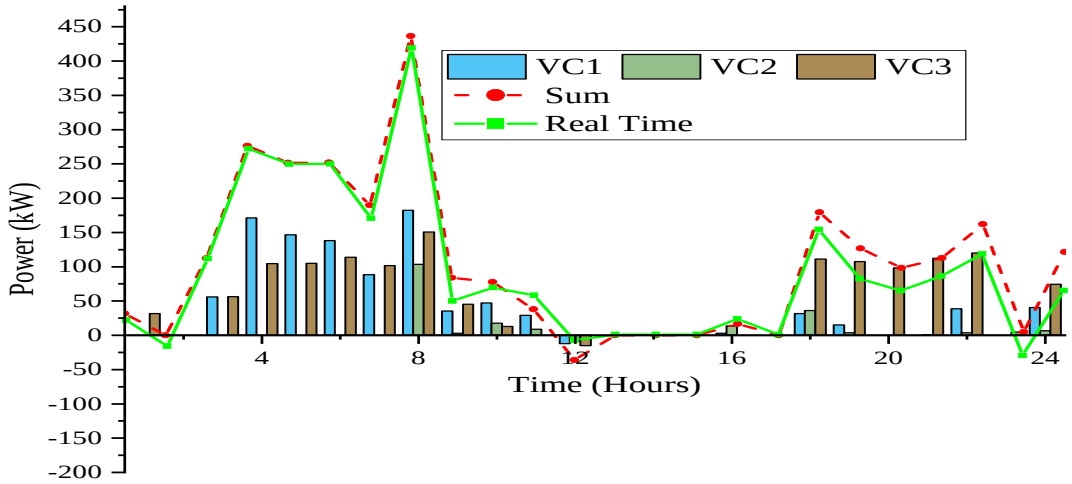

(c)

Figure 7.13: VC's Power Exchange with the Utility (a) *Case I*, (b) *Case II*, (c) *Case III*

Table 7.5: Cost ($) Assessment

	VC1				VC2				VC3			
	B_1	B_2	B_3	**Sum**	B_1	B_2	B_3	**Sum**	B_1	B_2	B_3	**Sum**
Case I	118.004	102.486	116.018	336.507	114.845	23.894	7.497	146.235	63.600	258.250	169.122	490.972
Case II	113.780	99.869	111.668	325.317	97.511	9.418	-10.578	96.351	60.783	248.335	162.329	471.448
Case III	94.187	84.505	91.534	270.226	75.311	-6.923	-34.477	33.911	54.257	231.105	150.046	435.408
*Case III**	93.60	83.77	91.24	268.61	73.55	-5.864	-37.26	30.43	46.04	193.43	131.07	370.55
Real Time	76.491	72.113	76.671	225.275	46.513	3.126	-11.770	37.869	79.451	174.106	131.183	384.740

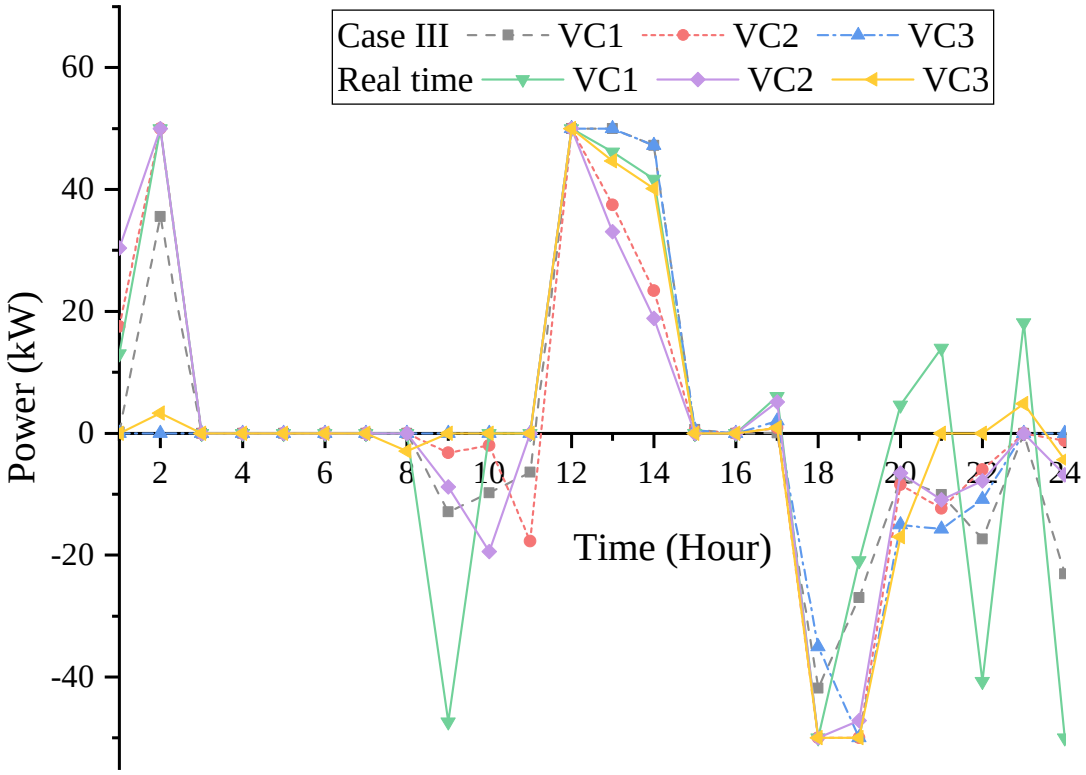

Figure 7.14: Charge/discharge power of BESSs

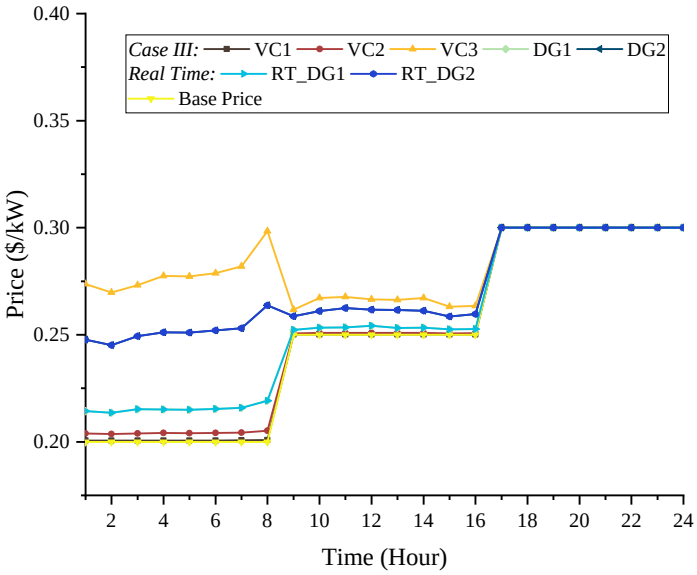

(a)

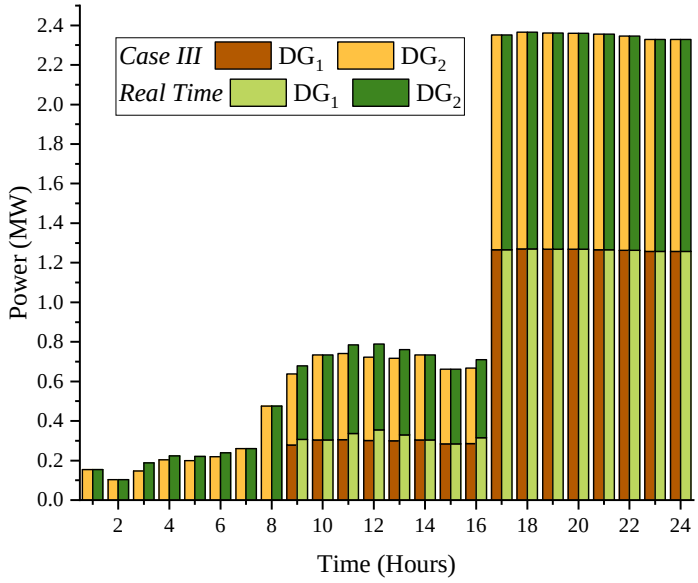

(b)

Figure 7.15: (A) LMP OF DIFFERENT BUSES CONTAINING THE ENTITIES IN DIFFERENT CASES AND VARIOUS PRICES, (B) POWER IMPORTED FROM DGS IN $Case\ III$ AND REAL TIME

A cost assessment among all the aforementioned cases is shown in Table 7.5. In $Case\ I$, for *VC1*, *VC2* and *VC3* the total cost is 336.507 \$, 146.235 \$, and 490.972 \$ respectively. Compared to the other cases, this cost is the highest. The reason behind this is that in $Case\ I$, the buildings operate autonomously by fulfilling their demand using RESs, load shifting, and solely engaging in energy trade with the utility. The RESs' efficiency in $Case\ II$ & $Case\ III$ is increased by the incorporation of energy exchange among buildings (B2B) and BESS. This statement is supported by the decline in power flow to/from the utility, as can be observed in Figure7.13. As an example, the power transferred to the utility by *VC2* during 1:00-3:00 hours is decreased compared to the base case. This decrease in energy is directed towards charging the battery to enable its subsequent utilization throughout the day, as illustrated in Figure 7.14. The charge and discharge of BESS are given in Figure 7.14. The B2B power exchanged and the cost involved is determined endogenously. Both sellers and buyers economically benefited from such energy exchange compared to that with the utility.

In order to see the effect of considering network constraints, the results of $Case\ III$ of this work and section 7.2 can be compared. The $Case\ III$ of section 7.2 is represented as $Case\ III^*$ in this section. The total cost of almost all the buildings is comparatively increased as can be seen from Table 7.5. The percentage increase in the total cost of each VC in $Case\ III$ with respect to that in section 7.2 is 0.6%, 11.44%, and 17.5%, respectively. The reason behind this is attributed to the usage of dynamic grid price and network utilization charges in this case compared to its earlier version.

Compared to $Case\ II$, the power supplied to the Grid is further decreased in $Case\ III$. This arises from the presence of inter-community (C2C) energy exchange in $Case\ III$ that enables the buildings to leverage load diversity across other busses. In Figure 7.13(c), it can be observed that the power exported to the utility for $Case\ III$ is insignificantly small. For *VC1, VC2* and *VC3* the overall cost is reduced by 16.93%, 64.80%, and 7.64% in $Case\ III$, relative to $Case\ II$. The respective C2C incentives for *VC1, VC2*, and *VC3* in $Case\ III$ are -22.151\$, 43.646\$, and -21.506\$ respectively.

The real-time simulation results have been plotted in the same graph as $Case\ III$'s results for a better comparison. The total power imported from the grid is almost the same as compared to $Case\ III$ except for certain hours, like around 18:00-20:00 hours, where import is reduced due to the availability of excess power in real-time than the day ahead. But this excess is not available with each building. The total cost of some buildings has been reduced in comparison

Table 7.6: VOLTAGE (P.U) IN REAL-TIME THROUGH SIMULATION AND RTDS

Bus no.	8^{th} Hour		20^{th} Hour	
	Simulation	**RTDS**	**Simulation**	**RTDS**
1	1.000	1.000	1.000	1.000
2	0.998	0.998	0.999	0.999
3	0.990	0.990	0.997	0.996
4	0.986	0.986	0.996	0.996
5	0.982	0.981	0.996	0.996
6	0.973	0.971	0.995	0.994
7	0.970	0.969	0.993	0.992
8	0.968	0.966	0.994	0.993
9	0.965	0.963	0.994	0.993
10	0.963	0.961	0.996	0.995
11	0.962	0.961	0.996	0.995
12	0.962	0.960	0.997	0.996
13	0.960	0.958	1.001	1.000
14	0.958	0.956	0.998	0.997
15	0.956	0.954	0.997	0.996
16	0.954	0.952	0.995	0.994
17	0.952	0.949	0.993	0.991
18	0.950	0.948	0.992	0.990
19	0.998	0.997	0.999	0.999
20	0.994	0.994	0.997	0.996
21	0.993	0.993	0.996	0.996
22	0.993	0.992	0.996	0.995
23	0.989	0.988	0.995	0.995
24	0.985	0.985	0.993	0.992
25	0.983	0.982	0.990	0.989
26	0.972	0.970	0.994	0.993
27	0.970	0.969	0.993	0.992
28	0.966	0.964	0.987	0.986
29	0.962	0.960	0.983	0.982
30	0.961	0.959	0.981	0.980
31	0.957	0.955	0.977	0.975
32	0.957	0.955	0.976	0.974
33	0.956	0.954	0.976	0.974

to that in $Case\ III$, as can be seen from Table 7.5. To manage the usage of BESS effectively, the receding horizon method [79] is used in real-time simulations that make the real-time BESS usage almost identical to that in $Case\ III$ as can be seen from Figure 7.14. The LMPs of various busses containing different entities have been given in Figure 7.15(a). The extra price for further increase in power demand in real-time is also shown in Figure 7.15(a). Table 7.6 shows the voltage of various busses during 8^{th} and 20^{th} hours. As can be seen from this Figure 7.15(a), during 8^{th} hour, the LMP increases abruptly for $18th$ bus containing $VC3$ due to the decrease in voltage to its limit, as can be seen in Table 7.6. The import of power from various DGs in real-time and $Case\ III$ is given in Figure 7.15(b), which are almost identical to each other.

This work has been validated through a real-time digital simulator (RTDS) as given in Appendix II. Table 7.6 shows a brief comparison between the simulation real-time result and RTDS results for two particular hours of consideration. Both the results are almost the same, which validates this work.

More buildings are integrated into different buses to test the scalability of the proposed work. Earlier, at buses 21, 24, and 18, we assumed $VC1$, $VC2$, and $VC3$, respectively. Similarly, these communities are replicated at buses 19, 10 and 5 as $VC4$, $VC5$, and $VC6$, respectively. Thus, this system consisted of 18 buildings. The total cost of all the six VCs in $CaseI$, $CaseII$, $CaseIII$, and $real-time\ case$ is found to be 1890.717\$, 1784.543\$, 1417.998\$, and 1392.094\$. Compared to the base case, there is a significant reduction in the cost of 5.616% and 25.002% in $CaseII$ and $CaseIII$, respectively. The cost in the real-time case does not have much variation in comparison to day-ahead scheduling ($CaseIII$). This savings in the total cost establishes the fact that this framework is scalable with the help of the concept of virtual communities.

In the proposed framework, day-ahead scheduling forms the baseline for real-time operations. The day-ahead schedule is determined based on forecasted data for renewable generation, load demand, and market prices. These schedules optimize energy transactions, including

- Day-ahead schedules calculate building-to-building (B2B), building-to-community (B2C), and community-to-community (C2C) energy exchanges.

- Charging and discharging schedules are optimized to store surplus renewable energy during off-peak hours and discharge it during peak demand periods.

- Adjusting load profiles in response to forecasted demand patterns.
- The schedule determines the quantity of energy imported from or exported to the utility grid.

In real-time operations, these day-ahead schedules act as baseline references but are adjusted dynamically to account for deviations caused by uncertainties in renewable generation or load demand. The real-time adjustments include

- Modifying charging/discharging schedules based on real-time renewable generation and demand fluctuations.
- Balancing discrepancies between scheduled and actual P2P transactions by importing/exporting energy from/to the grid.

Practical Example: Aggregated Profiles of Virtual Community 1 To illustrate this integration, the aggregated load, renewable generation, BESS charging/discharging, and grid exchange power profiles for Community 1 are analyzed as shown in Figure7.16. These graphs depict these profiles over a 24-hour period.

Day-Ahead Scheduling: During periods of high renewable generation (e.g., midday)(Figure 7.16(b)), surplus energy is stored in the BESS (Figure 7.16(c)) or traded with other communities/buildings via P2P transactions. During peak demand hours (around 1700 hours as shown in (Figure 7.16(a))), stored energy is discharged from the BESS to meet local demand or traded with other participants. Grid imports and exports are minimized as shown in Figure 7.16(d).

Real-Time Adjustments: The P2P (B2B and C2C) power exchanges are made fixed to the day-ahead values. If actual renewable generation (Figure 7.16(b)) exceeds forecasts, additional surplus energy is either stored in the BESS or exported to the grid. In case of lower-than-expected generation, additional energy is imported either from BESS (Figure 7.16(c)) or from the grid (Figure 7.16(d)).

The graphs (Figure 7.16) shows how day-ahead schedules align with forecasted trends while real-time adjustments ensure deviations are managed effectively. This integration ensures that day-ahead schedules provide a baseline while real-time adjustments maintain operational efficiency and reliability of the system. The practical example using virtual community 1's aggregated profiles highlights how this dual-stage approach optimizes energy management in a decentralized P2P trading framework. The candidate appreciates this opportunity to elaborate on this critical

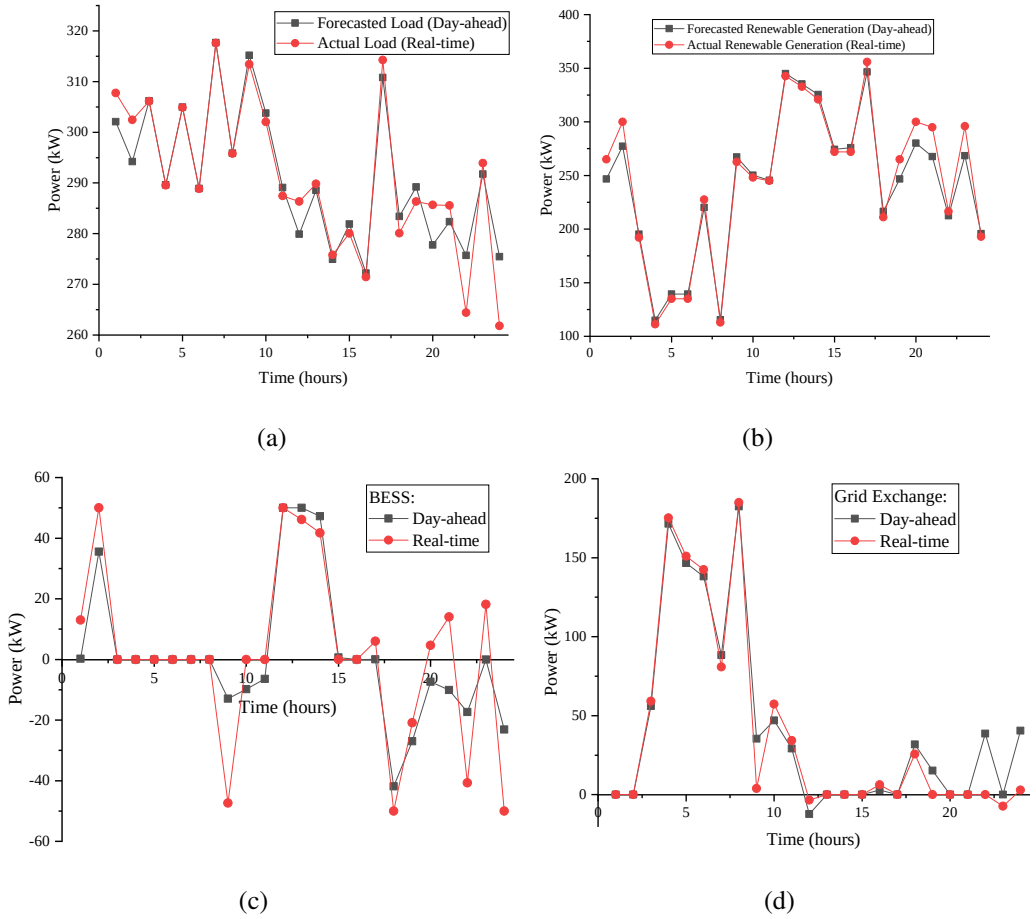

Figure 7.16: PRACTICAL EXAMPLE: AGGREGATED PROFILES OF VIRTUAL COMMUNITY 1 DURING DAY-AHEAD AND REAL-TIME OPERATION (A) LOAD PROFILE, (B) RENEWABLE GENERATION, (C) BESS CHARGING-DISCHARGING POWER PROFILE, AND (D) GRID EXCHANGE POWER PROFILE

aspect of the thesis and believes that this explanation clarifies the integration of day-ahead and real-time scheduling effectively.

This chapter presents a cooperative game based framework for economic benefit through P2P trading among buildings located at same or different bus. The proposed framework addresses the challenges of scalability by introducing the concept of virtual communities (VCs) to group buildings based on their location in the distribution system. This approach reduces the effective number of participants and transactions, thereby enhancing computational efficiency and scalability.

The framework incorporates three levels of energy trading: building-to-building (B2B) within a VC, building-to-community (B2C), and community-to-community (C2C). The use of a cloud computing platform facilitates P2P transactions without requiring direct data sharing between participants, enhancing privacy and potentially improving scalability. During real-time

scheduling, the buildings use day-ahead scheduling data for P2P energy exchange. Thus, in real-time scheduling, the complexity and burden on communication infrastructure reduces making it a more scalable approach.

Virtual communities group buildings into aggregated entities, effectively reducing the number of decision-making participants in P2P energy trading. This aggregation simplifies optimization by:

- Reducing transaction variables: Instead of individual buildings negotiating with all others, VCs act as intermediaries, lowering the number of bilateral interactions.
- Hierarchical decomposition: Complex large-scale problems are split into smaller sub-problems (intra-VC and inter-VC optimization).

In the context of this thesis, the advantages of this aggregation of buildings into virtual communities with quantitative comparisons are as follows.

- Transaction Volume Reduction: For 30 buildings grouped into 3 VCs
  - Without VCs: 30×29 = 870 potential B2B transactions.
  - With VCs: 3×2 = 6 C2C transactions + 10 intra-VC transactions per VC = 36 total transactions (approx 95% reduction).
- Parallelization: If there are n buildings total and m VCs, then there are approximately $\frac{n}{m}$ buildings in each VC. With parallelization, all three VCs can perform their intra-VC optimization at the same time. In the ideal case, the time required to solve the intra-VC optimization for all three VCs is approximately the same as the time required to solve the intra-VC optimization for one VC. If the sequential processing time is $3\times$ f($\frac{n}{m}$) and the parallel processing time is f($\frac{n}{m}$), then the parallel computation is approximately $\frac{1}{3}$ the time of the sequential processing. The reduction in computation is $\frac{(3-1)}{3} = \frac{2}{3}$, or about 66%. Thus, the parallelization reduces sequential computations by 66%. It is a very rough estimate based on the idea that the computation of all intra-VC optimizations can happen in parallel, significantly reducing the overall runtime.
- Data Aggregation: VCs share only net energy profiles with the DSO, avoiding individual building-level data exchange.

These results validate that virtual communities critically enhance scalability while preserving solution quality, making large-scale P2P energy trading computationally feasible. Overall, this thesis presents a more scalable approach to P2P energy trading that can accommodate a larger number of participants across diverse locations while maintaining computational efficiency and participant privacy.

7.4 Summary

This chapter presents a cost-saving framework for peer-to-peer (P2P) energy management for buildings grouped under Virtual Communities (VCs), which prevented the disclosure of any confidential information among the participants. The roles of prosumers as buyers or sellers are decided within the framework without any prior information regarding their energy surplus/deficit status. The modified Nash Bargaining method distributed the benefit appropriately among the participants. The total cost of all the buildings is increased by 10.45% as a result of the inclusion of grid constraints. The numerical analysis demonstrates the effectiveness of the proposed approach in harnessing the benefits of local P2P energy sharing. Compared to the base case, all three communities' combined total cost savings equals 24.05% in day-ahead scheduling. Load diversity among all buildings is leveraged, leading to a reduction in power exchange with the utility. Additionally, this framework adeptly handles uncertainties arising from Renewable Energy Sources (RESs) generation in the day-ahead and real-time energy markets with the help of BESS. To make the work more realistic, grid constraints are also incorporated with DGs participating actively in the energy market. The validation of results through RTDS enhances the feasibility of this work.